Ionospheric Research

NASA Grant No. NsG 134-61

Scientific Report

on

"An Investigation of Particle Penetration into the Magnetosphere"

by

T. E. Stevenson

February 10, 1967

Scientific Report No. 289

Ionosphere Research Laboratory

Submitted by: J. S. Nisbet (aw)

John S. Nisbet, Associate Professor of Electrical Engineering, Project Supervisor

Approved by: A. H. Waynick

A. H. Waynick, Director, Ionosphere Research Laboratory

The Pennsylvania State University

College of Engineering

Department of Electrical Engineering

TABLE OF CONTENTS

		Page
ABSTRACT		i
1.	INTRODUCTION	1
	1.1 General Statement of the Problem	1
	1.2 Previous Related Studies	1
	1.3 Present Knowledge of the Geomagnetic Field and the Solar Wind	7
	1.4 Penetration of Particles	11
	1.5 Specific Statement of the Problem	16
2.	TRAJECTORY OF A SINGLE CHARGED PARTICLE IN THE EQUATORIAL PLANE OF A TERMINATED DIPOLE	17
	2.1 Description of the Model	17
	2.2 Solution of the Equation of Motion	18
	2.3 Discussion of the Solution	28
3.	A CRITERION FOR THE TRAPPING OF CHARGED PARTICLES IN AN ARBITRARY TERMINATED MAGNETIC FIELD	35
	3.1 General Description of the Terminated Fields to be Discussed	35
	3.2 Development of the Criterion	37
	3.3 Extension of the Criterion to the Case of a Time-Varying Magnetic Field	43
	3.4 Discussion of the Results	52
4.	PARTICLE PENETRATION INTO A TERMINATED FIELD WHERE THE FIELD GRADIENT IS NOT PERPENDICULAR TO THE BOUNDARY	54
	4.1 Description of the Model	54
	4.2 Analog Simulation of the Equations of Motion	56
	4.3 Approximation of the Width of the Regions of the Indefinite Penetration by First Order Theory	70
5.	SUMMARY AND CONCLUSIONS	80
APPENDIX A		84
BIBLIOGRAPHY		86

ABSTRACT

A theoretical investigation is made of the trajectory of a solitary charged particle which emanates from free space and is incident at the boundary of an idealized magnetic field. The object is to arrive at some understanding of what is required of the magnetospheric field if charged solar particles, incident at the magnetospheric boundary, are to be prevented from being reflected back out of the magnetospheric cavity.

It is shown that reflection always occurs when a charged particle is incident near the equatorial boundary of a static terminated dipole field. Consequently, the Lorentz force equation and Newton's second law are used in an attempt to deduce some static and temporal, non-dipolar magnetic field variations required for deep penetration; emphasis is put on the case where the magnetic field gradient is perpendicular to the boundary.

Analog simulation and first order theory are then used to demonstrate that a charged particle may enter and penetrate deep within a magnetic field when the magnetic field gradient is not perpendicular to the boundary of the field. The model used is not meant to represent the field near the magnetospheric boundary. Indeed, at the present there is a lack of knowledge of this field on a sufficiently small spatial and time scale. Rather, the analysis is intended to demonstrate the feasibility of direct penetration across the magnetospheric boundary, in the event that the sufficient field variations do occur.

CHAPTER 1

INTRODUCTION

1.1 General Statement of the Problem

Recent space probes have revealed that the earth's magnetic field is confined within an elongated cavity due to the interaction of a solar plasma with the geomagnetic field. This plasma is generally thought to be a source of the charged particles responsible for such geophysical phenomena as the aurora polaris and the radiation belts. However, there is no generally accepted theory of how the charged solar particles enter and then become trapped in the earth's geomagnetic cavity.

This work is restricted to an analysis of the penetration and subsequent trapping of a single charged particle in some simplified models of this cavity. In addition, a review of some notable proposed mechanisms for particle penetration and trapping is included.

1.2 Previous Related Studies

Some of the first ideas linking certain geophysical phenomena with charged particles coming from outer space resulted from early investigations of magnetic storms. The early theories of magnetic storms usually attributed them to the action of something propagated from the sun to the earth. Lord Kelvin (1892) was able to show that these storms could not be the direct result

of variations in the sun's magnetic field, and Hale's (1913) measurements of the sun's field confirmed this. Consequently, the postulated solar agent became either ultraviolet radiation, or some corpuscular emission.

Birkeland's (1896) experiments lent credence to the "corpuscular" theories: he found that when he shot electrons toward a small magnetized sphere, many of the electrons were guided toward the polar regions. This provided the first insight into the magnetic disturbances in high latitudes, and into the aurora polaris.

Chapman and Ferraro (1931, 1932, 1933) suggested that essentially neutral clouds of ionized material were emitted from the sun during solar storms. They investigated the effect on the earth's magnetic field by using Maxwell's (1881) solution for the case of a dipole field parallel to, and approaching, a perfectly conducting sheet (see Figure 1). The solution shows that the induced currents in the perfectly conducting sheet cause the field to be confined to the side of the sheet adjacent to the dipole, and the field vanishes at two neutral points, Q, on the surface of the sheet (also see Dungey, 1958, pp. 137). Generalizing this result to the case of a neutral ionized stream approaching the earth's dipole field, Chapman and Ferraro concluded (1931, pp. 83):

> "In the case of a stream from the Sun advancing towards the Earth, a hollow space round the Earth is formed in the stream; the hollow is open at the back of the Earth (as viewed from the Sun)... part of the stream which has collected near the Earth re-

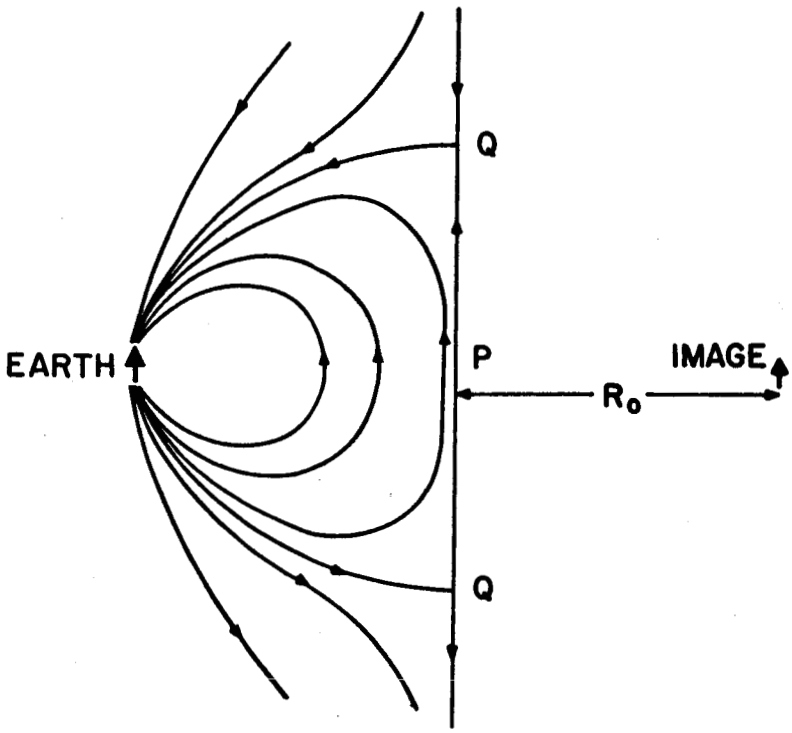

Figure 1. Field Configuration for a Dipole Parallel to, and Approaching, a Perfectly Conducting Sheet (Dungey, 1958).

> mains for a time, probably in the form of a ring round the equator; this gradually disappears by the passage of the ions and electrons, along the Earth's lines of force, into the atmosphere in high latitudes."

This was the beginning of the concept that a geomagnetic cavity is formed in an ionized stream of solar particles. However, since solar storms usually last for no more than three days, Chapman and Ferraro concluded that the geomagnetic cavity was only a temporary phenomenon.

Later, measurements of the zodiacal light by Allen (1946) and others (see Blackwell, 1956) indicated that there were electrons in all space in the vicinity of the sun at all times, but their density and the fashion in which they were moving could not be determined.

Biermann (1951) predicted that charged particles were being emitted continuously by the sun, not just in pulses as had been assumed by Chapman and Ferraro. He formed this conclusion after showing that photon radiation pressure alone was not enough to explain why comet tails always pointed away from the sun.

Theoretical studies by Parker (1958, 1960, 1963) and Chamberlain (1960) also indicated a continuous emission of solar particles. They showed that the solar corona was unstable and must be continually expanding outward in the form of a very low density plasma. Parker also arrived at plasma velocities and densities from coronal properties. In addition, he introduced the term "solar wind" in preference to the earlier terminology,

"solar corpuscular radiation," in order to emphasize that a stream of ionized solar material is blowing against the earth's magnetic field. Striking confirmations to the ideas and calculations of Biermann and Parker were given by interplanetary space probes in subsequent years.

Gringauz et al. (1960) detected interplanetary plasma fluxes of about 10^8 particles cm^{-2} sec^{-1} on Lunik 2 and 3. However, they could not differentiate between a light breeze and a solar wind, nor could they determine the direction of flow. Explorer 10 confirmed the Lunik fluxes, and, in addition, indicated that a definite wind came approximately from the sun with a velocity of about 300 km/sec (Bonetti et al., 1963).

Before the satellite era, Störmer (1955) proposed that charged particles emitted from the sun may impinge upon the earth's atmosphere after interacting with the geomagnetic field. He calculated many possible trajectories of a solitary charged particle in a dipole field, and presented a theoretical deduction of the locations of the auroral zones. However, his calculations with reasonable particle energies predicted higher auroral latitudes than are observed. His major assumptions were (1) that the earth's magnetic field was a dipole extending out to infinity, (2) that no interplanetary field existed, and (3) that the stream of solar particles was not neutral, but of one sign. However, recent space probes have suggested that the inaccuracy in Störmer's deduction of the locations of the auroral zones was due to

an oversimplification of the problem.

In view of the observational confirmation of the continual geomagnetic cavity by Explorers 10, 12, 14, 18 (Imp-1), and 21 (Imp-2), Störmer's use of a pure dipole field was a very crude approximation. In addition, field measurements on Pioneer 5 (Coleman et al., 1960) detected an interplanetary magnetic field of the order of a few gamma (1 gamma = 10^{-5} gauss).

The Mariner 2 spacecraft and the Imp-1 satellite have indicated that protons and He nuclei are present in the solar wind. Stormer's theory of the auroral zones had supposed the solar particles to be of one sign. However, since the required stream of charged particles of one sign would produce very large electric fields, it is now generally believed that the solar wind is neutral, at least on a macroscopic scale.

In addition to supplying data to confirm or deny theories about the long known polar phenomena, the satellites uncovered an entirely new magnetospheric phenomenon--the existence of geomagnetically trapped high energy particles (Van Allen, 1960). Innumerable subsequent probes confirmed the existence of two broad zones of penetrating particles: an outer zone where the energy appears mostly in the electrons, and an inner zone where it is primarily in the protons. The source of these particles is not known.

It is quite possible that the solar wind is at least one of the sources of the charged particles responsible for the aurorae

and the belts of geomagnetically trapped particles. But as of yet, there has been no generally accepted theory of how (or even whether) the solar wind penetrates into the earth's magnetic cavity. A major difficulty lies in the absence of sufficient knowledge of the magnetic field configuration, and in the corresponding lack of knowledge about the characteristics of the solar wind. In addition, it is not certain whether or not a geoelectric field exists, and, if so, what affects it has on the solar wind.

1.3 Present Knowledge of the Geomagnetic Field and the Solar Wind

Satellite investigations (see Cahill and Amazeen, 1963) have revealed that the geomagnetic field decreases radially within the geomagnetic cavity, as expected. But just outside the cavity, the magnetic field suddenly changes magnitude and starts wandering in direction and magnitude. The region inside the cavity is called the magnetosphere; the boundary of the cavity, termed the magnetopause, is located at about 10 earth radii in the direction of the sun, and at about 14 earth radii at 90 degrees to the sun-earth direction. Opposite to the sun, the cavity appears to increase to a cylinder with a radius of about 20 earth radii; this tail continues for a long distance, perhaps several earth-moon distances. Within the tail, the field is of the order of 20 to 30 gamma; near the edge of the magnetosphere on the noon

meridian, it is of the order of 40 to 80 gamma.

A thin current sheet in the tail, commonly referred to as the neutral sheet, was discovered by Ness (1965). It is about 600 km thick, and extends from about 10 earth radii out to beyond 40 earth radii in the tail. This sheet of east-west current separates the magnetic field in the northern section of the tail, which points toward the earth, from the southern section where the field points away from the earth.

In addition, Explorers 12 and 18 have detected the presence of a shock wave at about 14 to 16 earth radii on the dayside of the earth. This shock wave is formed in front of the magnetosphere because the velocity of the solar wind is greater than the Alfvén velocity, and is somewhat analogous to the shock wave formed by supersonic flow past a blunt body in gas dynamics.

The region between the shock wave and the magnetopause is referred to as the magnetosheath or transition region, and is experimentally characterized by a magnetic field which is turbulent compared to the field within the magnetosphere. Beyond the shock wave a small, slowly varying interplanetary field of about 4 gamma has been detected.

Figures 2 a and 2 b (from White, 1966) summarize what is presently known about the environment in the vicinity of the geomagnetic cavity.

It is now known (Bridge et al., 1965; IG Bulletin, 1964) that the solar wind is coming approximately radially from the sun

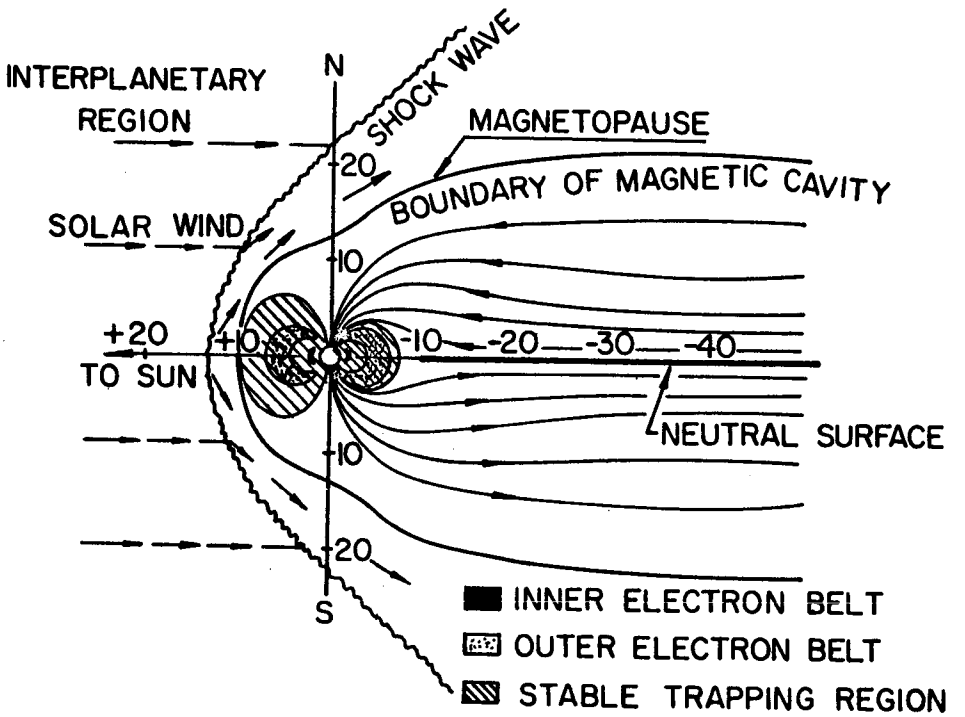

Figure 2a. Section Through the Magnetic Cavity (White, 1966).

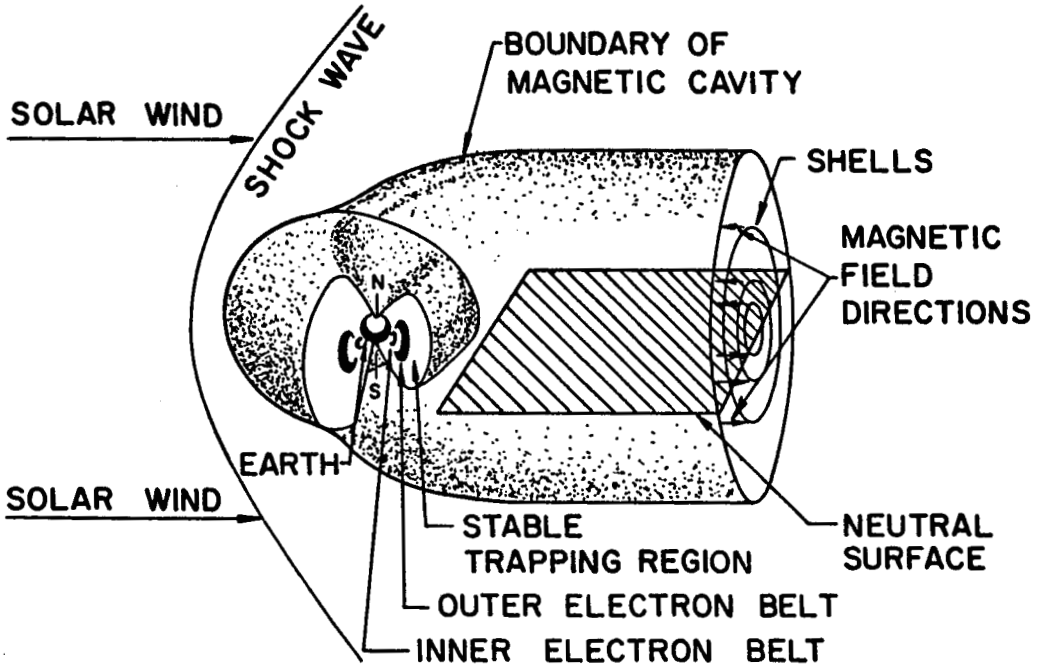

Figure 2b. The Magnetic Cavity (White, 1966).

with a velocity of about 300 to 500 km/sec, and the energy spread of the particles in the wind is narrow compared with the average directed energy ($\Delta E/E \tilde{=} 0.01$). In addition, the wind is very gusty, showing fluctuations in density, energy, and energy spread on a time scale of the order of hours.

While the solar wind is thought to be approximately neutral on a macroscopic scale, only protons and He nuclei have been detected. But without at least quasi-neutrality, unreasonably high electric fields would exist; thus electrons must also be present. Typical particle densities have been found to be of the order of 3 to 15 per cubic centimeter.

1.4 Penetration of Particles

The details of the magnetospheric boundary are of especial significance in the discussion of the source of particles inside the magnetosphere. In the first approximation, ionized particles can move only along a field line or through a point where there is no magnetic field. Whether these cases arise in one's theory depends upon the model of the magnetospheric boundary used. There are two general types of models which have been proposed so far: the closed model, and the open model.

In the closed model (see Figure 3), the earth's magnetic field is completely contained within the cavity. However, there are two neutral points (designated by N) corresponding to Chap-

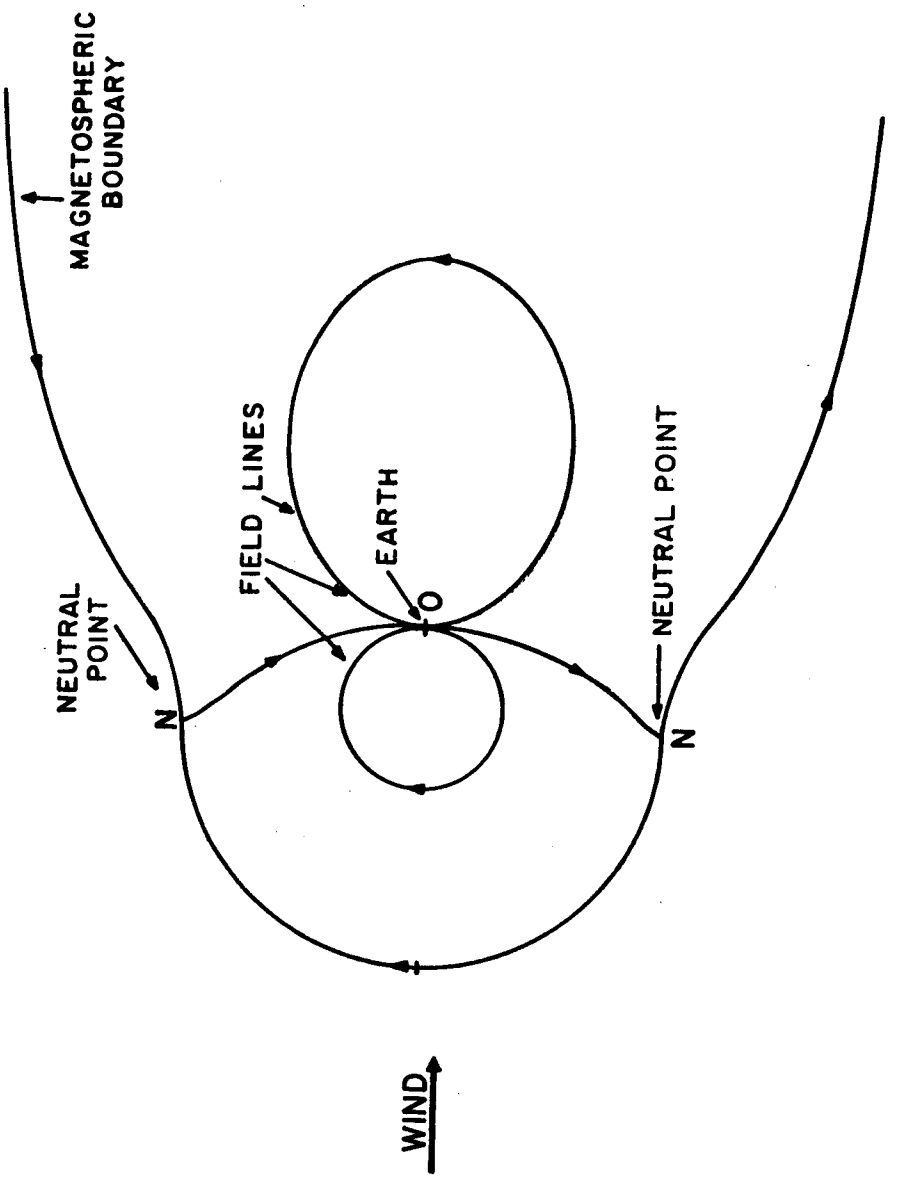

Figure 3. Closed Model of the Magnetosphere in a Meridian Plane Containing the Sun.

man and Ferraro's Q (see Figure 1). (In 3 dimensions, these are lines, not points.) Although the existence of an interplanetary magnetic field had been known, the magnitude was assumed to be negligibly small (see Dungey, 1954) in the development of this model. Blum (1963) presents a good review of the work leading up to the closed model, as well as an extensive bibliography.

With the discovery of a regular interplanetary magnetic field by Pioneer 5, Dungey (1961) developed the open model of the magnetosphere. The main feature of the open model is that some geomagnetic field lines are connected with the interplanetary field. Figure 4 is a sketch of the model for the case of a southward interplanetary field. In this particular case, there are two neutral points (designated by N), one on the front and the other on the tail of the cavity.

In both models, charged solar particles impinging at the neutral points may travel unimpeded along the lines of force which connect the neutral points to the earth. In the open model, however, charged particles may also enter the magnetosphere by spiraling along the field lines which connect the geomagnetic field to the interplanetary field.

In both cases the locations of the neutral points are such as to suggest a mechanism for the source of auroral particles only. The idea of particle penetration at a neutral point is not new, however. As a result of his observations of solar flares,

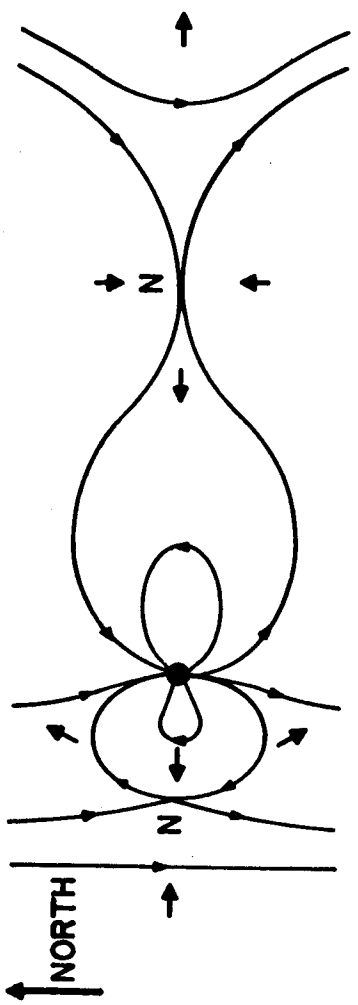

Figure 4. Open Model of the Magnetosphere in a Meridian Plane Containing the Sun. Bold Arrows Refer to Plasma Flow, Small Arrows Show Magnetic Field Directions. N Designates Neutral Points.

Giovanelli (1947) suggested that discharges of charged particles should occur at neutral points in a magnetic field. Hoyle (1949) first suggested that neutral points may be responsible for the primary auroral particles. Dungey (1958) extended Hoyle's ideas by arguing that not only should a discharge occur at a neutral point, but that individual particles can gain energy at the expense of the bulk flow.

As pointed out by Dungey (1961), in the case of the open model, if the interplanetary field is directed northward, the surface of the lines of force enclose the earth, but it does not meet the earth. Consequently, in this case, no auroral zones are generated. He therefore concluded that there is an approximate southward interplanetary field. Speiser (1964) presents a detailed discussion of the formation of neutral points and an analysis of particle trajectories passing through the neutral points.

The effectiveness of particle penetration along the field lines in an open model, as a source of particles in the magnetosphere, is not yet known. It is currently being studied by Grebowsky (1966) at the Pennsylvania State University. However, it is apparent from Figure 4 that this should be principally a polar cap phenomenon.

Thus, neither model of the magnetosphereic boundary gives a steady source of low latitude particles as an obvious effect. One must look further at the magnetospheric boundary for a source of such particles.

1.5 Specific Statement of the Problem

One source of low latitude particles, as well as even possibly auroral particles, may be a penetration across the magnetospheric boundary. This work is concerned with such a source. In particular, it is concerned with the motion of a solitary charged particle which emanates from a field-free region and is incident at the boundary of a magnetic field. Some simple models of both static and time-varying magnetic fields will be considered.

CHAPTER 2

TRAJECTORY OF A SINGLE CHARGED PARTICLE IN THE EQUATORIAL PLANE OF A TERMINATED DIPOLE

2.1 Description of the Model

From Figure 2 it is seen that the earth's magnetic field is largely confined to the interior of the magnetosphere. On the dayside of the earth near the equatorial plane, the field configuration of the interior of the magnetosphere may be approximated by that of a static magnetic dipole. If, in addition, it is assumed that no magnetic field exists on the sunside of the magnetopause, the geomagnetic field near the equatorial plane can be given approximately by the terminated dipole (using spherical coordinates)

$$\bar{B} = -(K/r^3)(2\cos\theta\,\bar{a}_r + \sin\theta\,\bar{a}_\theta),\quad r \leq r_o \sin^2\theta, \qquad (2.1)$$

$$= 0 \qquad\qquad r > r_o \sin^2\theta,$$

where $r_o = 10\, r_e$ (earth radii)

$\tilde{=} 6.3 \times 10^7$ meters

and K is the earth's dipole moment (8.1×10^{15} weber-meter).

In order to gain some insight into the problem of particle penetration near the equatorial zone of the magnetosphere, the equations of motion will now be solved for the case of a single

charged particle which is incident at the equatorial boundary of the terminated dipole given by Equation (2.1).

2.2 Solution of the Equation of Motion

In spherical coordinates relative to the center of the terminated dipole (see Figure 5), the velocity of the charged particle is given by

$$\overline{V} = V_\theta \overline{a}_\theta + V_\phi \overline{a}_\phi + V_r \overline{a}_r, \text{ for all } r. \tag{2.2}$$

The particle is assumed to be traveling at a constant velocity in the free space, in the equatorial plane, before impinging on the terminated dipole at (r_o, ϕ_c). Without loss of generality, it shall be required that $\overline{V}$ be perpendicular to the line connecting $(r_o, 0)$ to (r_o, π) for $r \geq r_o$, and that $\pi \leq \phi_o \leq 2\pi$. Therefore,

$$\overline{V}(r_o, \phi_o) = V_{o\phi} \overline{a}_\phi + V_{or} \overline{a}_r, \tag{2.3}$$

where $\phi_o = 3\pi/2 - \arctan(V_{o\phi}/V_{or})$,

$$V_\theta = 0, \; r \geq r_o,$$

and where $V_{o\phi}$ and V_{or} are constants.

By using the Lorentz force equation, $\overline{F} = q(\overline{V} \times \overline{B})$, and Newton's second law, $\overline{F} = d(m\overline{V})/dt$, together with Equation (2.2) and Equation (2.1) for $r \leq r_o \sin^2 \theta$, one may arrive at the following three equations by equating vector components:

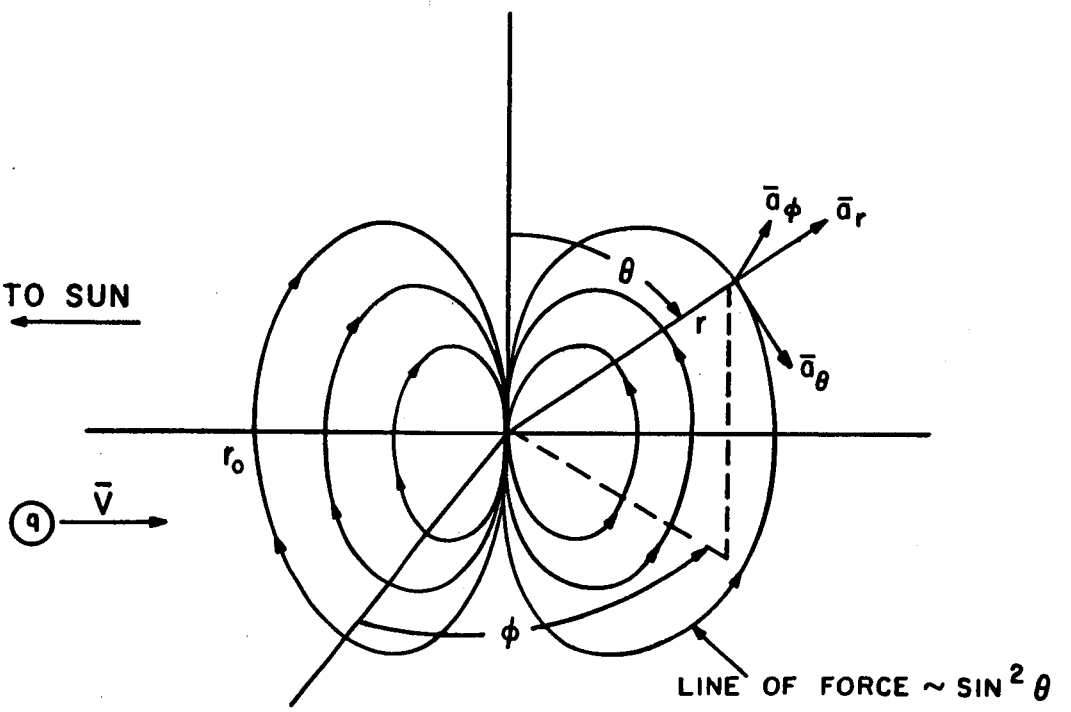

Figure 5. Static Terminated Dipole Representation of the Earth's Magnetic Field.

$$(b/r^3)\,(V_r \sin\theta - 2\,V_\theta \cos\theta) = dV_\phi/dt, \tag{2.4}$$

$$2(b/r^3)\,V_\phi \cos\theta = dV_\theta/dt, \tag{2.5}$$

$$-(b/r^3)\,V_\phi \sin\theta = dV_r/dt, \tag{2.6}$$

where $b = -(q/m)\,K$

and (q/m) is the charge-to-mass ratio of the particle.

In using Newton's second law, relativistic effects drop out since dm/dt is zero for all velocities when the only applied force is purely magnetic; this is proved in Appendix A.

Also proved in Appendix A is the fact that $|\overline{V}|^2$ is a constant. Therefore, by Equations (2.2) and (2.3),

$$V_{o\phi}^2 + V_{or}^2 = V_\theta^2 + V_\phi^2 + V_r^2, \text{ for all } r. \tag{2.7}$$

The particle is assumed to have no initial velocity in the $\overline{a}_\theta$ direction. The only way to impart a velocity component in the $\overline{a}_\theta$ direction is by the interaction (cross product) of the radial field with the velocity component in the $\overline{a}_\phi$ direction. But there is no radial field component in the equatorial plane of the terminated dipole. Therefore, V_θ must always be zero, and θ must always be 90 degrees.

Consequently, Equation (2.6) reduces to

$$-(b/r^3)\,V_\phi = dV_r/dt \tag{2.8}$$

and Equation (2.7) yields

$$V_\phi = \pm \sqrt{(V_{o\phi}^2 + V_{or}^2) - V_r^2}. \qquad (2.9)$$

Combining Equations (2.8) and (2.9) gives

$$\mp (b/r^3) \sqrt{(V_{o\phi}^2 + V_{or}^2) - V_r^2} = dV_r/dt. \qquad (2.10)$$

By using the chain rule for derivatives, together with the relationships

$$V_\phi = r\,(d\phi/dt), \qquad \text{for } \Theta = 90^\circ,$$

and

$$V_r = dr/dt,$$

one readily finds that

$$dV_r/dt = V_r\,(\partial V_r/\partial r) + (V_\phi/r)\,(\partial V_r/\partial \phi). \qquad (2.11)$$

By using Equations (2.9) and (2.11) in (2.10), one obtains

$$\mp (b/r^3) \sqrt{(V_{o\phi}^2 + V_{or}^2) - V_r^2} = V_r\,(\partial V_r/\partial r)$$

$$\pm (1/r) \sqrt{(V_{o\phi}^2 + V_{or}^2) - V_r^2}\,(\partial V_r/\partial \phi). \qquad (2.12)$$

After rearranging terms in Equation (2.12), and noting that $\partial V_r/\partial V_r = 1$, one arrives at the following expression:

$$0 = r^3 V_r (\partial V_r/\partial r) \pm \sqrt{(V_{o\phi}^2 + V_{or}^2) - V_r^2}\; r^2(\partial V_r/\partial \phi)$$

$$\pm b\sqrt{(V_{o\phi}^2 + V_{or}^2) - V_r^2}\; (\partial V_r/\partial V_r). \quad (2.13)$$

In order to solve (2.13), it may be noted that by applying the chain rule for differentials to dV_r, and again using the relationship $\partial V_r/\partial V_r = 1$, the following equation may be found.

$$0 = dr(\partial V_r/\partial r) + d\phi(\partial V_r/\partial \phi) - dV_r(\partial V_r/\partial V_r). \quad (2.14)$$

Next, consider three vectors which are defined as follows:

$$\bar{Z}_1 = dr\,\bar{a}_r + d\phi\,\bar{a}_\phi - dV_r\,\bar{a}_v, \quad (2.15)$$

$$\bar{Z}_2 = (\partial V_r/\partial r)\,\bar{a}_r + (\partial V_r/\partial \phi)\,\bar{a}_\phi + (\partial V_r/\partial V_r)\bar{a}_v, \quad (2.16)$$

$$\bar{Z}_3 = r^3 V_r\,\bar{a}_r \pm \sqrt{(V_{o\phi}^2 + V_{or}^2) - V_r^2}\; r^2\,\bar{a}_\phi$$

$$\pm b\sqrt{(V_{o\phi}^2 + V_{or}^2) - V_r^2}\; \bar{a}_v, \quad (2.17)$$

where $\bar{a}_r$, $\bar{a}_\phi$, $\bar{a}_v$ are the unit vectors in (r, ϕ, V_r)-space. Note that Equation (2.13) implies

$$\bar{Z}_3 \cdot \bar{Z}_2 = 0 \quad (2.18)$$

and Equation (2.14) implies

$$\bar{Z}_1 \cdot \bar{Z}_2 = 0. \quad (2.19)$$

The solution of Equation (2.13) in (r, ϕ, V_r)-space is a surface, $V_r(r, \phi)$. In addition, $\overline{Z}_2$ is the gradient of this surface. By Equations (2.18) and (2.19), $\overline{Z}_1$ and $\overline{Z}_3$ are both normal to the gradient, $\overline{Z}_2$. Since the whole surface $V_r(r, \phi)$ is a solution to Equation (2.13), and since $\overline{Z}_1$ and $\overline{Z}_3$ are both normal to the gradient of the surface, $\overline{Z}_2$, it is possible to generate a point on the surface by requiring that $\overline{Z}_1$ be parallel to $\overline{Z}_3$ at that point. Consequently, the corresponding vector components of $\overline{Z}_1$ and $\overline{Z}_3$ must be proportional at that point, and the following equation may be written.

$$\frac{dr}{r^3 V_r} = \pm \frac{d\phi}{r^2\sqrt{(V_{o\phi}^2 + V_{or}^2) - V_r^2}} = \pm \frac{dV_r}{b\sqrt{(V_{o\phi}^2 + V_{or}^2) - V_r^2}} . \tag{2.20}$$

By Equation (2.20), after rearranging terms, one finds that

$$\frac{dr}{r^3} = \mp \frac{V_r\, dV_r}{b\sqrt{(V_{o\phi}^2 + V_{or}^2) - V_r^2}} . \tag{2.21}$$

Therefore,

$$\int \frac{dr}{r^3} = \mp \int \frac{V_r\, dV_r}{b\sqrt{(V_{o\phi}^2 + V_{or}^2) - V_r^2}} - \frac{C_o}{2} . \tag{2.22}$$

Integrating Equation (2.22) and rearranging the terms gives

$$\pm\sqrt{(V_{o\phi}^2 + V_{or}^2) - V_r^2} = \frac{b}{2}\left(C_o - \frac{1}{r^2}\right). \qquad (2.23)$$

The required boundary condition is that

$$V_r(r_o, \phi_o) = V_{or}. \qquad (2.24)$$

Therefore, by Equations (2.23), (2.24), and (2.9),

$$C_o = \frac{2}{b} V_{o\phi} + \frac{1}{r_o^2}, \qquad (2.25)$$

where $V_{o\phi}$ may be positive, negative, or zero.

By substituting Equation (2.25) into Equation (2.23) and rearranging terms, one finds that

$$V_r(r, \phi_o) = \pm\left[(V_{o\phi}^2 + V_{or}^2) - \left\{\frac{b}{2}\left(\frac{2}{b} V_{o\phi} + \frac{1}{r_o^2} - \frac{1}{r^2}\right)\right\}^2\right]^{\frac{1}{2}}. \qquad (2.26)$$

The minus (-) sign applies when the particle is traveling toward the dipole, and the plus (+) sign applies when the particle is traveling away from it.

By Equation (2.26), $V_r(r, \phi_o) = 0$ when $r = r_p$, where

$$r_p = \frac{r_o}{\sqrt{\pm (2r_o^2/b)(V_{o\phi}^2 + V_{or}^2)^{1/2} + (2r_o^2/b) V_{o\phi} + 1}}. \qquad (2.27)$$

In order to satisfy the requirement that $r_p \leq r_o$, the plus (+) sign in Equation (2.27) is used when the charge is negative, and the minus (-) sign is used when the charge is positive.

Note that for $r < r_p$, $V_r(r, \phi_o)$ becomes imaginary. Therefore, r_p is the closest radial position to the dipole center which the charged particle may penetrate.

Figure 6 illustrates the behavior of $V_r(r, \phi_o)$ for the case of a charged particle which has a non-zero initial radial component of velocity. Initially, $V_r(r, \phi_o) = V_{or}$, a negative quantity; then, as the arrowheads indicate, as r approaches close to r_p, $V_r(r, \phi_o)$ increases algebraically. At $r = r_p$, $V_r(r, \phi_o) = 0$; but the radial component of velocity cannot remain equal to zero indefinitely because $d V_r(r_p, \phi_o)/dt \neq 0$, according to Equation (2.10). Therefore, $V_r(r, \phi_o)$ must become positive and the particle must move in a positive radial direction. At $r = r_o$, $V_r(r, \phi_o) = -V_{or}$ (a positive quantity), as shown in Figure 6. Consequently, since the radial velocity of the particle cannot drop discontinuously to zero at the boundary of the equitorial plane of the terminated dipole, the particle must enter back into free space.

For the case of a positively charged particle where $V_{o\phi} > 0$ and $V_{or} \rightarrow 0$, $r_p \rightarrow r_o$ by Equation (2.27). Therefore, the trajectory of the particle is merely a straight line which is tangential to the boundary of the terminated dipole.

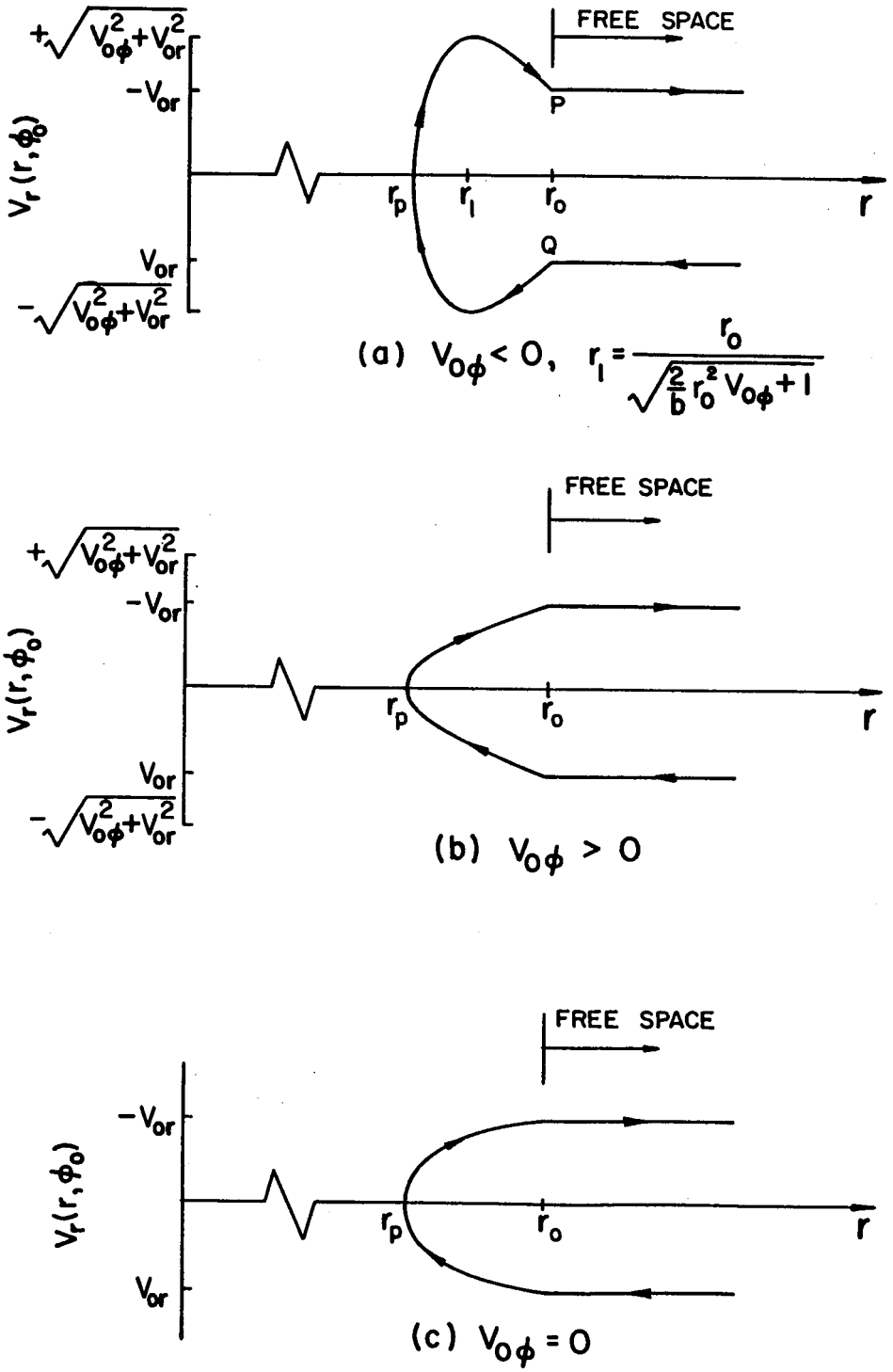

Figure 6. Behavior of $V_r(r, \phi_o)$ for the Case of a Positive Charge with a Non-zero Initial Radial Component of Velocity. Inequalities are Reversed for the Case of a Negative Charge.

And, for the case of a positively charged particle where $V_{o\,\phi} < 0$ and $V_{or} \rightarrow 0$, points P and Q both approach $(r_o, 0)$ in Figure 6 (a). But, in the limit, as $V_{or} \rightarrow 0$, the particle must be reflected back into free space since $V_r(r, \phi_o)$ must be continuous.

A similar analysis holds for the case of a negatively charged particle. The conclusion, therefore, is that no charged particle, regardless of sign of charge, energy, or mass, can become trapped in the equatorial plane of a static terminated dipole.

The actual trajectory may be found by calculating $\phi(r)$. Let (r_p, ϕ_p) be the coordinates of the point of the trajectory closest to the center of the dipole. By Equation (2.20)

$$\int_{\phi_o}^{\phi} d\phi = \int_{V_r(r_o)}^{V_r(r)} -\frac{r^2}{b}\, dV_r. \tag{2.28}$$

By substituting the differential, dV_r, from Equation (2.21) into Equation (2.28) and integrating, one finds that

$$\phi(r) = \begin{cases} G(r) - G(r_o) + \phi_o, & \text{where } r_o \geq r \geq r_p, \text{ such that } r \rightarrow r_p; \\ 2\,G(r_p) - G(r_o) - G(r) + \phi_o, & \text{where } r_p \leq r \leq r_o, \text{ such that } r \rightarrow r_o, \end{cases} \tag{2.29}$$

where

$$G(r) = \frac{1}{\sqrt{\frac{4\, r_{ox}^{4}\, V_{ox}^{2}}{b^{2}}}} \log_e \left\{ \sqrt{-\frac{1}{4} + \frac{r^2}{2\, r_{ox}^{2}} + \left(\frac{V_{ox}^{2}}{b^{2}} - \frac{1}{4\, r_{ox}^{4}} \right) r^4} + r^2 \sqrt{\frac{V_{ox}^{2}}{b^{2}} - \frac{1}{4\, r_{ox}^{4}}} + \frac{1}{\sqrt{\frac{4\, r_{ox}^{2}\, V_{ox}^{2}}{b^{2}} - 1}} \right\}$$

$$-(1/2) \arcsin \left\{ - \left[b/(2 \mid v_{ox} \mid^{1/2}) \right] (1/r_{ox}^{2} - 1/r^{2}) \right\},$$

where r_{ox} and V_{ox} are defined as follows:

$$1/r_{ox}^{2} = (2/b)\, V_{o\phi} + 1/r_{o}^{2}$$

$$V_{ox}^{2} = V_{o\phi}^{2} + V_{or}^{2}.$$

Figure 7 is a sketch of several possible trajectories of a single charged particle of constant energy.

2.3 Discussion of the Solution

As explained earlier, and demonstrated by the use of Figures 6 and 7, if a single charged particle emanates from free space and travels in the equatorial plane of a static terminated dipole, such that it is incident to the dipole field anywhere along

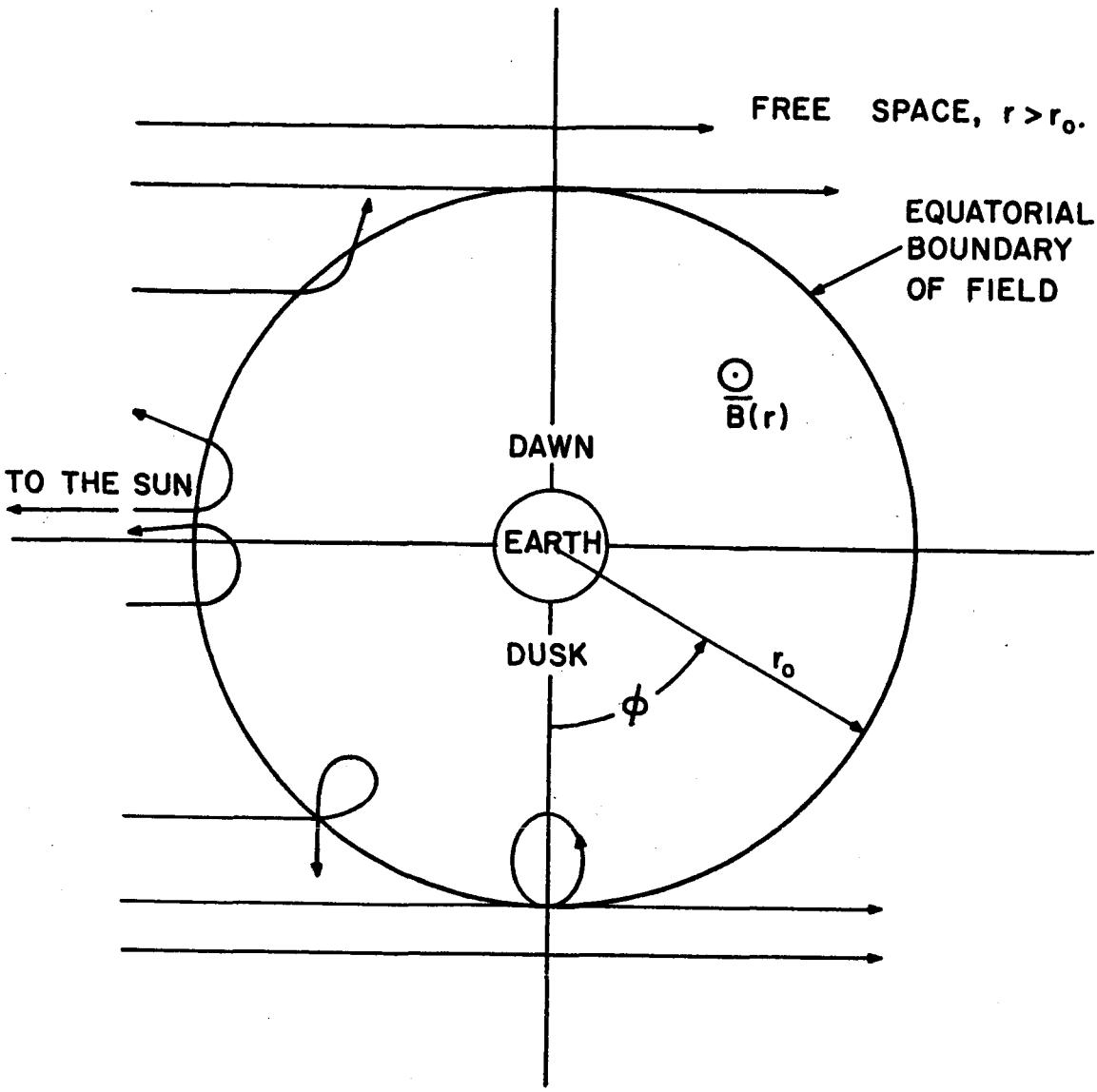

Figure 7. Schematic of Electron Penetration in the Equatorial Plane of a Static Terminated Dipole.

the equatorial boundary, it will be completely reflected back into free space. For further discussion, it will be helpful to determine the maximum depth of radial penetration when the particle is restricted to move in the equatorial plane.

According to Equation (2.27), the furthest radial penetration is given by

$$r_p = \frac{r_o}{\sqrt{1 + C}} \tag{2.30}$$

where

$$C = \frac{2 r_o^2}{b} \left\{ \pm (V_{o\phi}^2 + V_{or}^2)^{1/2} + V_{o\phi} \right\}. \tag{2.31}$$

As before, the plus (+) sign in Equation (2.31) is used when the charge is negative, and the minus (-) sign is used when the charge is positive. It may be shown that $C \ll 1$ when the particle is an electron or a proton whose energy is less than 100 kev. Therefore, by using the binomial expansion of Equation (2.30), one finds that

$$r_p \tilde{=} \frac{r_o}{1 + C/2}, \quad C \ll 1. \tag{2.32}$$

Let Δ_p be defined as the maximum radial distance which the particle may penetrate into the static terminated dipole. That is,

$$\Delta_p \equiv r_o - r_p. \tag{2.33}$$

Therefore, for $C \ll 1$, by Equations (2.33), (2.32), and (2.31),

$$\Delta_p = \frac{(V_{o\phi}^2 + V_{or}^2)^{1/2}}{(b/r_o^3)} \left\{ \pm 1 + \frac{V_{o\phi}}{(V_{o\phi}^2 + V_{or}^2)^{1/2}} \right\}. \tag{2.34}$$

By substituting $b = -(q/m)\,K$ into Equation (2.34), and noting that $\cos \phi_o = V_{o\phi}/(V_{o\phi}^2 + V_{or}^2)^{1/2}$, one obtains

$$\Delta_p \begin{cases} = r_L (1 + \cos \phi_o), \text{ for an electron,} \\ \\ = r_L (1 - \cos \phi_o), \text{ for a proton,} \end{cases}$$

where

$$r_L = \frac{(V_{o\phi}^2 + V_{or}^2)^{1/2}}{|\, q/m \,|\, (K/r_o^3)}. \tag{2.35}$$

In Equation (2.35), r_L is the Larmor radius of the charged particle in a magnetic field of magnitude K/r_o^3, the magnitude of the field along the equatorial boundary of the static terminated dipole. By Equation (2.35), the maximum radial distance which a particle of a given energy may penetrate varies from zero to $2\,r_L$, depending upon the incident coordinate angle, ϕ_o. Figure 8 is a polar plot of the behavior of Δ_p as a function of ϕ_o, for the case of an electron. The plot for the case of a proton is similar, except that the curve $\overset{\frown}{R\text{-}S\text{-}T}$ is rotated 180° about the line con-

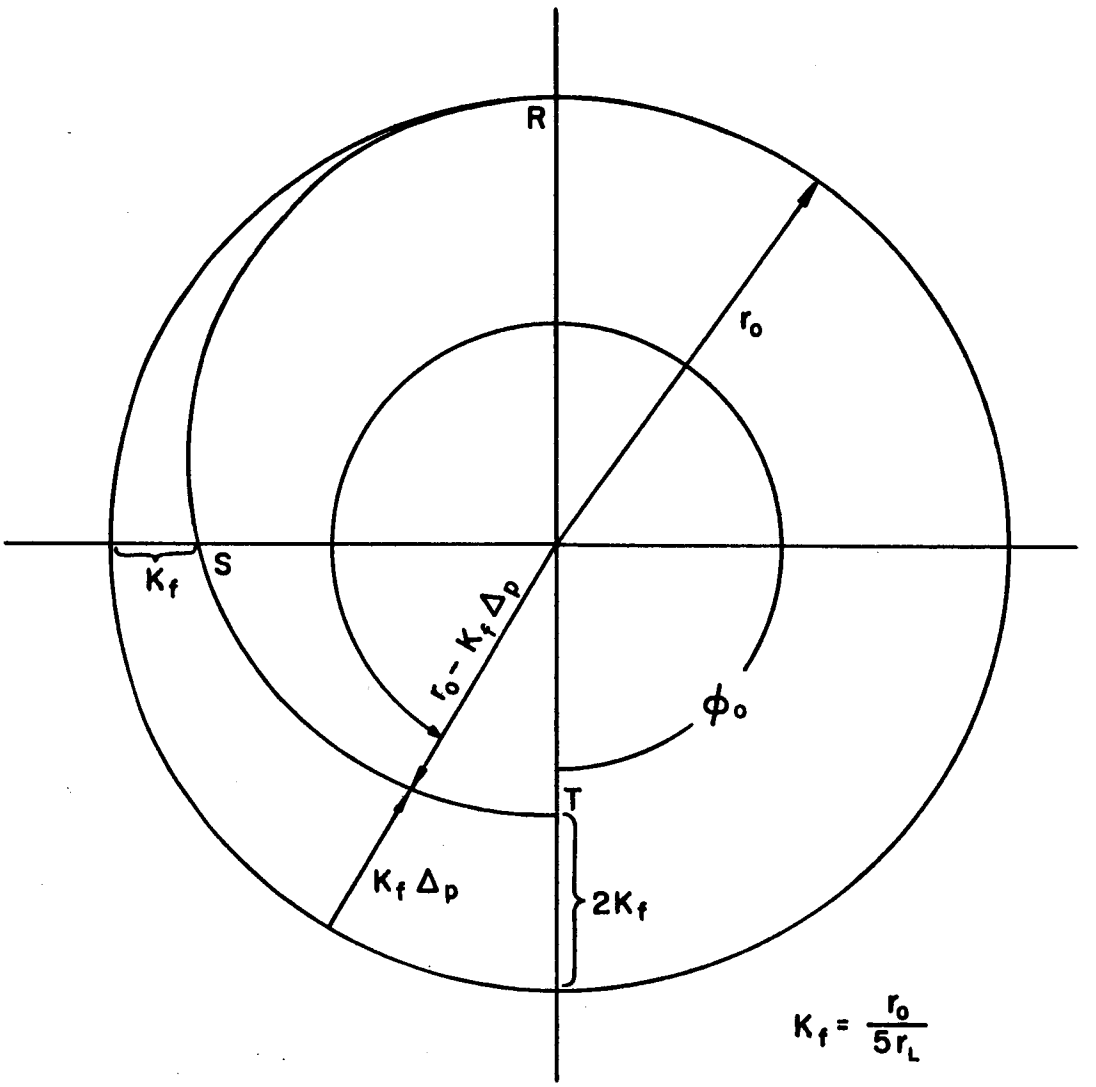

Figure 8. Polar Plot of the Behavior of Δ_p as a Function of the Coordinate Angle of Incidence, ϕ_o, for the Case of an Electron.

necting $(r_o, 3\pi/2)$ to the origin, $(0, \phi)$.

For a 100 kev electron, $r_L = 32$ km, and for a 100 kev proton, $r_L = 1375$ km; in both cases, $r_L \ll r_o$. Consequently, since a charged particle penetrates radially into the terminated dipole for a distance of $2\ r_L$ at most, the particle experiences a very small change in magnetic field during the course of its trajectory within the dipole field. This fact may be used to discuss qualitatively the motion of a charged particle which is incident off the equatorial plane, or at an angle to this plane. The motion of the particle may be resolved into two components, one along a field line and one perpendicular to it. As long as the velocity along the field line is not too high, the small Larmor radius means that the particle has little time to spiral along a field line before again reaching the boundary of the terminated dipole. The conclusion, therefore, is that reflection occurs everywhere in the general equatorial region. The motion of a particle which is incident near the poles is more complicated, but will not be considered because the magnetosphere is so unlike the terminated dipole at high latitudes.

It may therefore be concluded that if the interplanetary field is ignored, the dipolar variation of the magnetosphere near the equatorial region of the sunside of the magnetopause is insufficient to account for particle trapping alone. Consequently, if charged particles which are incident near the equatorial zone are to be trapped by the geomagnetic field, it appears that

either temporal or non-dipolar spatial variations of the geomagnetic field, or both, are an important aspect of the trapping mechanism. In addition, since $r_L \ll r_o$ for electrons and protons of energy less than 100 kev, the curvature of the magnetopause on the sunside of the earth has little effect on the trajectory of such charged particles. So, in order to investigate some possible mechanisms which may contribute to the trapping of charged particles, one may simply consider a straight magnetospheric boundary when investigating the problem from a single particle approach.

CHAPTER 3

A CRITERION FOR THE TRAPPING OF CHARGED PARTICLES IN AN ARBITRARY TERMINATED MAGNETIC FIELD

3.1 General Description of the Terminated Fields to be Discussed

As a consequence of the results of Chapter 2, the possibility of particle trapping in the equatorial region will be investigated by considering the motion of a charged particle which is incident at the boundary of a more general magnetic field that is bordered, at least in part, by free space. The object is to deduce some general properties required of a static terminated magnetic field which will allow the particle to penetrate deep within the field, rather than be reflected back into free space.

Two specific types of terminated magnetic fields will be considered; namely, (1) a field configuration which has a circular boundary and is given by (using spherical coordinates)

$$\overline{B} = B_\theta (r, \phi)\, \overline{a}_\theta, \quad r \leq r_o, \tag{3.1}$$

$$= 0 \quad , \quad r > r_o,$$

and (2) a semi-infinite field region which has a straight boundary and is given by (using Cartesian coordinates)

$$\overline{B} = B_z(x, y)\,\overline{a}_z \quad , \quad y \geq 0, \qquad (3.2)$$

$$= 0 \quad , \quad y < 0.$$

In the first case, indefinite penetration will be said to occur when a solitary charged particle, emanating from free space, impinges upon the boundary of the field with a non-zero initial radial component of velocity--and continues to move within the field with a net motion directed toward the origin of the coordinate system (wherever that may be). This would correspond to charged particles penetrating through the magnetospheric boundary and moving toward the upper atmosphere of the earth.

In the second case, indefinite penetration will be defined as occurring when the particle impinges upon the boundary of the field with a positive component of velocity in the $\overline{a}_y$-direction--and continues moving within the field with a net motion directed away from the boundary.

Indefinite penetration may be regarded as being synonymous with trapping in the case of a static terminated field; but, as illustrated in Section 3.3, in the case of a time-varying terminated field, trapping may occur without indefinite penetration.

The case involving the straight boundary is included in addition to that with the circular boundary, because, as explained in Chapter 2, if the Larmor radius of the particle is small compared to the curvature of the boundary of the field, the boundary appears to be essentially straight. However, the

criterion for indefinite penetration in both cases turns out to be similar.

3.2 Development of the Criterion

First consider the terminated magnetic field given by Equation (3.2). If a particle impinges upon the field with a component of velocity in the third (i.e., parallel to $\bar{a}_z$) direction, that component stays constant since it is parallel to the field. Therefore, that component may be disregarded as far as trapping is concerned, and the velocity of the particle will be given by

$$\bar{V} = V_x \bar{a}_x + V_y \bar{a}_y, \text{ for all } x, y. \tag{3.3}$$

And, at the point of incidence, $(x_o, 0)$,

$$\bar{V}(x_o, y_o) = V_{ox} \bar{a}_x + V_{oy} \bar{a}_y, \; V_{oy} > 0, \tag{3.4}$$

where V_{ox} and V_{oy} are constants.

By using the Lorentz force equation, $\bar{F} = q(\bar{V} \times \bar{B})$, and Newton's second law, $\bar{F} = d(m\bar{V})/dt$, together with Equation (3.3) and Equation (3.2) for $y \geq 0$, one may arrive at the following two equations by equating vector components:

$$-(q/m)\, B_z\, V_x = dV_y/dt, \tag{3.5}$$

$$(q/m)\, B_z\, Y_y = dV_x/dt, \tag{3.6}$$

where (q/m) is the charge-to-mass ratio of the particle.

In a manner similar to the way equation (2.26) was derived in Chapter 2, one may use (3.3), (3.4), and (3.5) to obtain

$$V_y = \pm \left[(V_{ox}^2 + V_{oy}^2) - \left\{ (q/m) \int_0^y B_z\,(x,\, y)\, dy + V_{ox} \right\}^2 \right]^{1/2} . \tag{3.7}$$

The plus (+) sign in Equation (3.7) is used when the particle is traveling in the positive $\bar{a}_y$-direction, and the minus (-) sign is used when the particle travels in the opposite direction--that is, back toward the boundary. In taking the integral in (3.7), x is kept constant since x, y, and V_y are treated as independent variables in the derivation of (3.7).

Initially, the $\bar{a}_y$-component of velocity is positive. Therefore, one obvious sufficient condition for indefinite penetration of a particle of given charge, mass, and energy is that $B_z(x, y)$ be such that

$$(V_{ox}^2 + V_{oy}^2) > \left\{ (q/m) \int_0^y B_z\,(x,y)\, dy + V_{ox} \right\}^2 \tag{3.8}$$

for all $y > 0$.

If $B_z\,(x,\, y)$ is such that for a given charged particle of

given energy, there exists a $y = y_p$ such that

$$(V_{ox}^2 + V_{oy}^2) = \left\{ (q/m) \int_0^{y_p} B_z(x,y)\, dy + V_{ox} \right\}^2, \tag{3.9}$$

then $V_y(x, y_p) = 0$, and the particle may or may not reverse its motion in the $\bar{a}_y$-direction, depending upon that particular $B_z(x, y)$. Even if the particle does reverse direction at some such point, that does not mean it will not be able to stay within the field by again reversing its motion at yet another point. A familiar example where this may occur is when the gradient of the field is small over a Larmor radius, so that the particle motion may be described by the motion of its guiding center; since the particle moves about its guiding center with a cyclotron motion, the actual motion of the particle reverses periodically in the $\bar{a}_y$-direction, even though the velocity of the guiding center may always have a component along the positive $\bar{a}_y$-direction. This particular example will be studied in more detail, with the aid of an analog computer, in Chapter 4.

While Equation (3.7) cannot be used to describe the general character of the field required for indefinite penetration, it can be used to determine if a particular static field will absolutely not allow indefinite penetration. For instance, one immediate result of Equation (3.7) is that if B_z is a function of y only, and if, in addition, it is a monotonically increasing

or decreasing function of y, then complete reflection will occur. This is true because there will exist a point $y = y_p$ where $V_y = 0$; and since the integral of B_z (y) appears within a bracket that is squared, and V_y is required to be continuous, the particle will be reflected back into free space.

However, if B_z (y) undergoes sign reversals with increasing y, it is apparent that (3.8) may be fulfilled for all y; thus the particle may penetrate the field indefinitely, or at least until the amplitude of B_z (y) becomes too large.

If B_z (y) is of the form $B_o \cos(ky)$, then for a given B_o, and a given charged particle of specified energy, (3.8) may be satisfied by making k large enough. For example, if $V_{ox} = 0$, and $B_z(y) = B_o \cos(ky)$, then in order to (3.8) to be satisfied it shall be required that k be such that

$$V_{oy} > \left| (q/m)(B_o/k) \right| . \tag{3.10}$$

That is,

$$k > 1/r_L ,$$

where

$$r_L = \frac{V_{oy}}{\left| (q/m) B_o \right|} \tag{3.11}$$

is the Larmor radius of the charged particle in a constant magnetic of magnitude $| B_o |$. Near the boundary of the equatorial zone of the magnetosphere, on the sunside of the earth, the

magnetic field is of the order of 3×10^{-8} weber/m^2. For the case of $B_o = 3 \times 10^{-8}$ weber/m^2, $r_L = 32$ km for a 100 kev electron, and $r_L = 1375$ km for a 100 kev proton. Therefore, for $V_{ox} = 0$, it is required that

$$k > 3 \times 10^{-5} \text{ m}^{-1}, \text{ for a 100 kev electron,}$$

and

$$k > 7.3 \times 10^{-7} \text{ m}^{-1}, \text{ for a 100 kev proton,}$$

in order for (3.8) to be satisfied in the case where $B_z(y) = 3 \times 10^{-8}$ weber/m^2 cos (ky). And for a given type of charged particle, the required value of k increases as the energy of the incident particle is reduced.

In light of the preceding discussion, it appears that if B_z is a function of y only, and if it may be approximated over a region as a Fourier series, then indefinite (or at least deep) penetration is more likely to occur if the coefficients of the dominant harmonic terms, B_k, are related to the corresponding harmonics, k, by the expression

$$k > | (q/m) B_k | / V_{oy}. \qquad (3.12)$$

More generally, it may be stated that in the case of the magnetosphere, it appears that if the gradient of the field is perpendicular to the boundary, and if large non-monotonic vari-

ations in this field occur over a Larmor radius, then particle penetration into the magnetosphere may be enhanced. As an example of the distance over which such a large variation is required, it should be about 32 km for a 100 kev electron and about 1375 km for a 100 kev proton; the variation must occur over shorter distances for lower energy electrons and protons.

For the case of a solitary charged particle impinging upon the terminated field given by (3.1), one finds that the radial component of velocity is given by

$$V_r = \pm \left[(V_{o\phi}^2 + V_{or}^2) - \left\{ (q/m) \int_{r_o}^{r} B_\theta (r, \phi)\, dr + V_{o\phi} \right\}^2 \right]^{1/2}, \tag{3.13}$$

where $r \leq r_o$.

Equation (3.13) may be found by substituting $B_\theta (r, \phi)$ for K/r^3 in Equations (2.8) through (2.21), and solving for V_r. As in Equation (2.26), $V_{o\phi}$ and V_{or} are the components of velocity in the $\bar{a}_\phi$- and $\bar{a}_r$-direction, respectively, at the point of incidence, (r_o, ϕ_o), along the boundary of the field. In evaluating the integral in (3.13), ϕ is kept constant since r, ϕ, and V_r are treated as independent variables in the development of the equation.

Since (3.13) is of the same form as (3.7), conclusions similar to those involving $B_z (y)$ may be found for $B_\theta (r)$ by substituting r for y, and ϕ for x, in the previous discussion of $B_z (y)$ in (3.7).

3.3 Extension of the Criterion to the Case of a Time-Varying Magnetic Field

The object here is to investigate the trajectory of a single charged particle which emanates from free space and is incident at the boundary of the static field given by (3.14) and shown by the solid line in Figure 9. Then the effect of allowing the field distribution to vary, as shown by the dashed line in Figure 9, will be investigated by the use of (3.13). The static field is given by

$$B_\theta(r) = \begin{cases} 2K_1(r_m - r), & 0 \leq r \leq r_m; \\ -2K_2(r_m - r), & r_m \leq r \leq r_c; \\ 2K_3(r_o - r), & r_c \leq r \leq r_o; \\ 0, & r > r_o, \end{cases} \tag{3.14}$$

where K_1, K_2, and K_3 are all positive constants.

By Equations (3.13) and (3.14) for $r_c \leq r \leq r_o$,

$$V_r = \pm \left[(V_{o\phi}^2 + V_{or}^2) - \left\{ -(q/m) K_3 (r_o - r)^2 + V_{o\phi} \right\}^2 \right]^{1/2}, \tag{3.15}$$

where $r_c \leq r \leq r_o$. Initially, at $r = r_o$, $V_r = V_{or} < 0$. Therefore, if

$$(V_{o\phi}^2 + V_{or}^2) > \left\{ -(q/m) K_3 (r_o - r)^2 + V_{o\phi} \right\}^2 \tag{3.16}$$

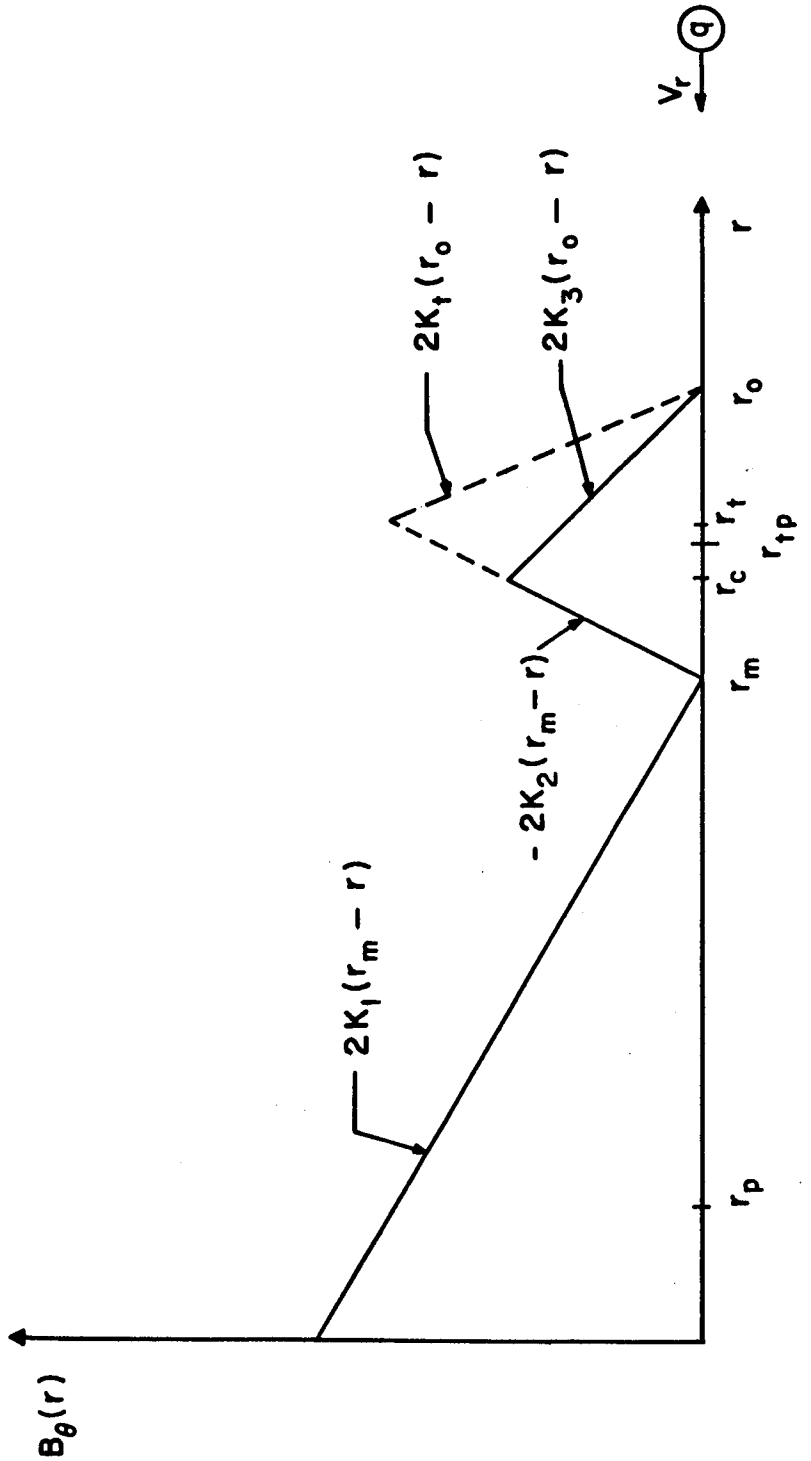

Figure 9. Radially Dependent Field Configuration. Solid Line Shows the Initial Field; Dashed Line Indicates the Temporal Variation over the Interval $r_c \leq r \leq r_o$.

for $r_c \leq r \leq r_o$, then $V_r < 0$ for $r_c \leq r \leq r_o$, and the charged particle will penetrate the field radially to at least r_c. For a 40 kev proton, for example, $(V_{o\phi}^2 + V_{or}^2)$ equals $(2.76 \times 10^6$ m/sec$)^2$; so if $V_{o\phi} = 1 \times 10^6$ m/sec, for instance, then (3.16) may be fulfilled if $K_3 (r_o - r_c) = 3 \times 10^{-8}$ weber/m^2 and $(r_o - r_c) = 1000$ km. (However, if $(r_o - r_c) > 1400$ km, then V_r will become equal to zero somewhere along the interval $r_c < r < r_o$, and the proton will be reflected back into free space, as illustrated by Figure 10.)

Suppose the inequality in (3.15) is met. Then, by (3.13) and (3.14) for $r_m \leq r \leq r_o$,

$$V_r = \pm \left[(V_{o\phi}^2 + V_{or}^2) - \left\{ -(q/m) K_3 (r_o - r_c)^2 + (q/m) K_2 \left((r_c - r_m)^2 - (r - r_m)^2 \right) + V_{o\phi} \right\}^2 \right]^{1/2}, \quad (3.17)$$

where $r_m \leq r \leq r_c$. Again, if

$$(V_{o\phi}^2 + V_{or}^2) > \left\{ -(q/m) K_3 (r_o - r_c)^2 + (q/m) K_2 \left((r_c - r_m)^2 - (r - r_m)^2 \right) + V_{o\phi} \right\}^2 \quad (3.18)$$

for $r_m \leq r \leq r_c$, then the particle will continue to penetrate radially to at least r_m. The inequality in (3.18) will be met for the case of a 40 kev proton, for example, if $(r_c - r_m) =$

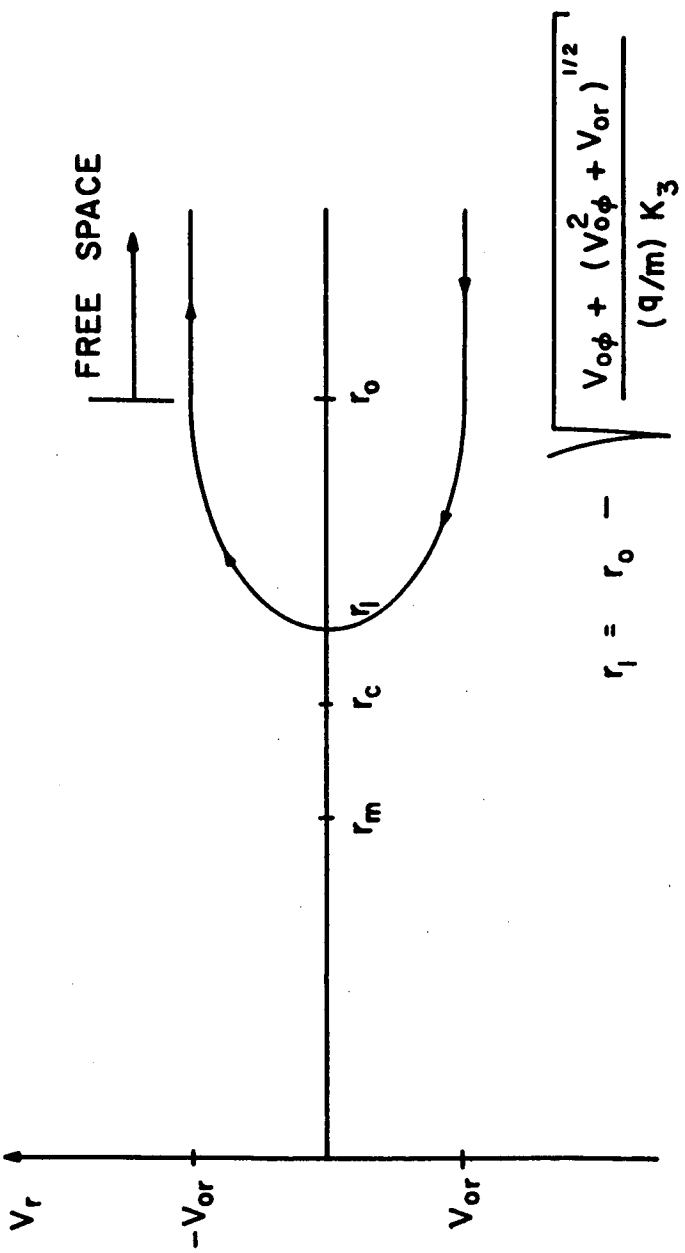

Figure 10. Behavior of V_r When $(r_o - r_c) < 1400$ km.

500 km, and the rest of the parameters are as were previously prescribed for (3.16) to hold. (If, on the other hand, $(r_c - r_m) >$ 1700 km, V_r will become equal to zero somewhere along the interval $r_m < r < r_c$, and the proton will be reflected back into free space.)

Suppose the inequality in (3.18) holds. Then, by (3.13) and (3.14) for $0 \leq r \leq r_o$,

$$V_r = \pm \left[(V_{o\phi}^2 + V_{or}^2) - \left\{ -(q/m) K_3 (r_o - r_c)^2 + (q/m) K_2 (r_c - r_m)^2 - (q/m) K_1 (r_m - r)^2 + V_{o\phi} \right\}^2 \right]^{1/2}, \tag{3.19}$$

where $0 \leq r \leq r_m$. Now suppose that there exists $r = r_p$, where $0 < r_p < r_m$, such that $V_r = 0$. Such would be the case for a 40 kev proton if, for example, $r_o = 10\ r_e$ (earth radii), $K_1 > 6 \times 10^{-7}$ weber/m^3, and the rest of the parameters are as were prescribed for (3.16) and (3.18) to hold. Then the particle will reverse its radial motion at r_p and eventually be reflected back into free space, as illustrated by Figure 11. Consequently, no trapping occurs in this particular static field configuration.

However, suppose that once the particle has passed the radial coordinate r_c with a negative radial velocity, the field changes as indicated by the dashed line in Figure 9. Then, as in the static case, if $V_r = 0$ at $r = r_p$, where $0 < r_p < r_m$, the

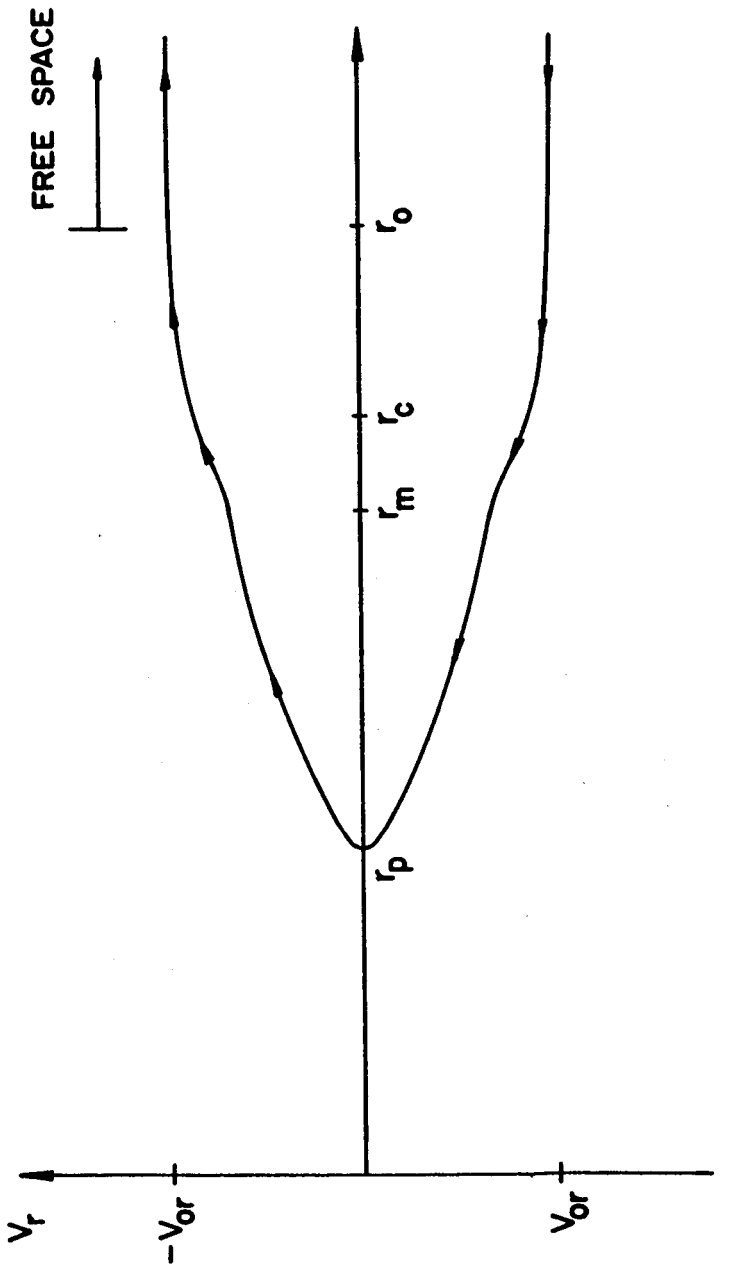

Figure 11. Behavior of V_r When $(r_o - r_c) < 1400$ km, $(r_c - r_m) < 1700$ km, and $K_1 > 6 \times 10^{-7}$ weber/m^3.

particle's radial motion will reverse and it will move toward r_t, where $r_c < r_t < r_o$ (see Figure 9). As the particle moves from r_p toward r_c, Equation (3.19) will still apply for $r_p \leq r \leq r_m$, and (3.17) will apply for $r_m \leq r \leq r_c$ (where the positive signs are used in both cases). However, an expression for the radial component of velocity must be determined anew for $r_c \leq r \leq r_t$ and for $r_t \leq r \leq r_o$; this may be done as follows.

Equation (3.13) applies for any terminated field where the spherical coordinate system is located within the field, and where the field vanishes for $r > r_o$. In addition, $(V_{o\phi}^2 + V_{or}^2)$ is a constant. Therefore, if a field-free region of infinitesimal radial thickness is assumed to exist in the neighborhood of r, where $r_c \leq r \leq r_t$, (3.13) may be applied by replacing the definite integral by an indefinite integral plus a constant of integration, C_t, and by replacing $V_{o\phi}$ by $V_{ot\phi}$. Here $V_{ot\phi}$ may be interpreted as the component of velocity in the $\bar{a}_\phi$-direction which the particle has when it reaches the infinitesimal field-free region in the neighborhood of r. Therefore, one may write

$$V_r = \pm \left[(V_{o\phi}^2 + V_{or}^2) - \left\{ (q/m) \int (-2 K_2 (r_m - r)) \, dr + C_t + V_{ot\phi} \right\}^2 \right]^{1/2}, \tag{3.20}$$

where $r_c \leq r \leq r_t$.

One may determine the quantity $(C_t + V_{ot\phi})$ by the requirement that

$$V_r(r_c^-) = V_r(r_c^+), \tag{3.21}$$

where $V_r(r_c^-)$ is found by setting $r = r_c$ in (3.17), and $V_r(r_c^+)$ is determined by setting $r = r_c$ in (3.20). After performing these substitutions, one finds that

$$C_t + V_{ot\phi} = -(q/m) K_3 (r_o - r_c)^2 - (q/m) K_2 (r_c^2 - 2r_m r_c) + V_{o\phi}. \tag{3.22}$$

Therefore, by Equations (3.20) and (3.22), one finds that

$$V_r = \pm \Bigg[(V_{o\phi}^2 + V_{or}^2) - \Big\{ -(q/m) K_3 (r_o - r_c)^2 + (q/m) K_2 \Big[(r_m - r)^2 - (r_m - r_c)^2 \Big] + V_{o\phi} \Big\}^2 \Bigg]^{1/2}, \tag{3.23}$$

where $r_c \leq r \leq r_t$.

Now if

$$(V_{o\phi}^2 + V_{or}^2) > \Big\{ -(q/m) K_3 (r_o - r_c)^2 + (q/m) K_2 \Big[(r_m - r)^2 - (r_m - r_c)^2 \Big] + V_{o\phi}^2 \Big\}^2 \tag{3.24}$$

for $r_c \leq r \leq r_t$, then the particle will continue moving radially into the interval $r_t \leq r \leq r_o$. If, however, $V_r = 0$ at some $r = r_{tp}$, where $r_c < r_{tp} < r_t$, then the particle will become trapped within the field and will continue to move radially between r_{tp} and r_p as long as field distribution between r_t and r_o is as shown by the dashed line in Figure 9. Such would be the case for the previously discussed 40 kev proton if $(r_t - r_m) \geq$ 1100 km, and the rest of the parameters are as were prescribed for (3.16) and (3.18) to hold. The time interval over which the required variation in field must take place for such trapping, is of the order of half a Larmor period of the proton, evaluated at the average field experienced by the proton. If the average field is 3×10^{-8} weber/m^2, for instance, then the Larmor period of the proton is about 2.2 seconds. Therefore, if $(r_t - r_m) = 1100$ km, the field maximum on the interval $r_c \leq r \leq r_o$ must approximately double over a period of the order of one second.

If, on the other hand, (3.24) holds, then one may determine V_r for $r_t \leq r \leq r_o$, in a manner similar to the way (3.23) was derived. It turns out that

$$V_r = \pm \Bigg[(V_{o\phi}^2 + V_{or}^2) - \Big\{ -(q/m) K_3 (r_o - r_c)^2 + (q/m) K_2 \left[(r_m - r_t)^2 - (r_m - r_c)^2 \right] + (q/m) K_t \left[(r_o - r_t)^2 - (r_o - r)^2 \right] + V_{o\phi} \Big\}^2 \Bigg]^{1/2}, \quad (3.25)$$

where $r_t \leq r \leq r_o$, and K_t is defined in Figure 9. If $V_r = 0$ for some $r = r_{op}$, where $r_t \leq r_{op} \leq r_o$, then the particle will become trapped in the field. But if $V_r \neq 0$ over the interval $r_t \leq r \leq r_o$, then the charged particle will enter back into free space. Again, in the case of the 40 kev proton, using the same parameters as were prescribed for (3.16) and (3.18) to hold, if $(r_t - r_m) \geq$ 700 km, then trapping will take place. If $(r_t - r_m) = 700$ km, the maximum of the field must therefore increase by 40 per cent, which is about 60 per cent less than the increase required for trapping in the interval $r_c \leq r \leq r_t$; however, the period over which the increase must occur is still about the same order of magnitude.

3.4 Discussion of the Results

According to (3.12), it appears that if the gradient of the magnetospheric field is perpendicular to the magnetospheric boundary, then particle penetration into the cavity may be enhanced if large, non-monotonic variations occur in the field over a Larmor radius. In addition, rapid temporal variations (occuring over a period of the order of a Larmor period) are seen to be sufficient for the enhancement of particle penetration. However, such temporal fluctuations appear to be too rapid to actually occur in the case of the magnetosphere.

The bulk of the material in this chapter was devoted to

the special case where the gradient of the field is normal to the boundary of a terminated magnetic field. The case where the gradient is at an angle to the boundary will be the subject of Chapter 4, where the analog computer will be used to supplement the ideas developed in this chapter. While (3.7) and (3.13) offer some suggestions for the nature of the field required for particle trapping in the equatorial region of the magnetosphere, they are limited in that the trajectory must be calculated for the case when the field varies in two dimensions. This is a difficult task to perform without the use of approximations or a computer.

CHAPTER 4

PARTICLE PENETRATION INTO A TERMINATED FIELD WHERE THE FIELD GRADIENT IS NOT PERPENDICULAR TO THE BOUNDARY

4.1 Description of the Field

Chapters 2 and 3 dealt primarily with particle penetration into terminated field configurations where the field gradient was normal to the field boundary. In Chapter 2 it was shown that a static terminated dipole field caused a single charged particle, incident near the equatorial zone of the dipole, to be reflected back into free space; consequently, in Chapter 3, an attempt was made to deduce some static and time-varying, non-dipolar field variations required for deep particle penetration and trapping, with emphasis on the case where the field gradient was perpendicular to the boundary.

In the present chapter the case where the field gradient is not normal to the boundary will be considered. The object is to investigate how particle penetration into an arbitrary static terminated field is affected by (1) the energy of the particle, (2) the angle of incidence of the particle, (3) the scale of the field, and (4) by the angle between the field gradient and the boundary. The static terminated magnetic field to be investigated is illustrated in Figure 12, and given by (using Cartesian coordinates)

$$B_z(X,Y) = B_{ox}(K_x X + 1) + B_{oy}(K_y Y + 1) \ , \quad Y \geq 0 \ ,$$

$$B_z(X,Y) = 0 \ , \quad Y < 0 \ .$$

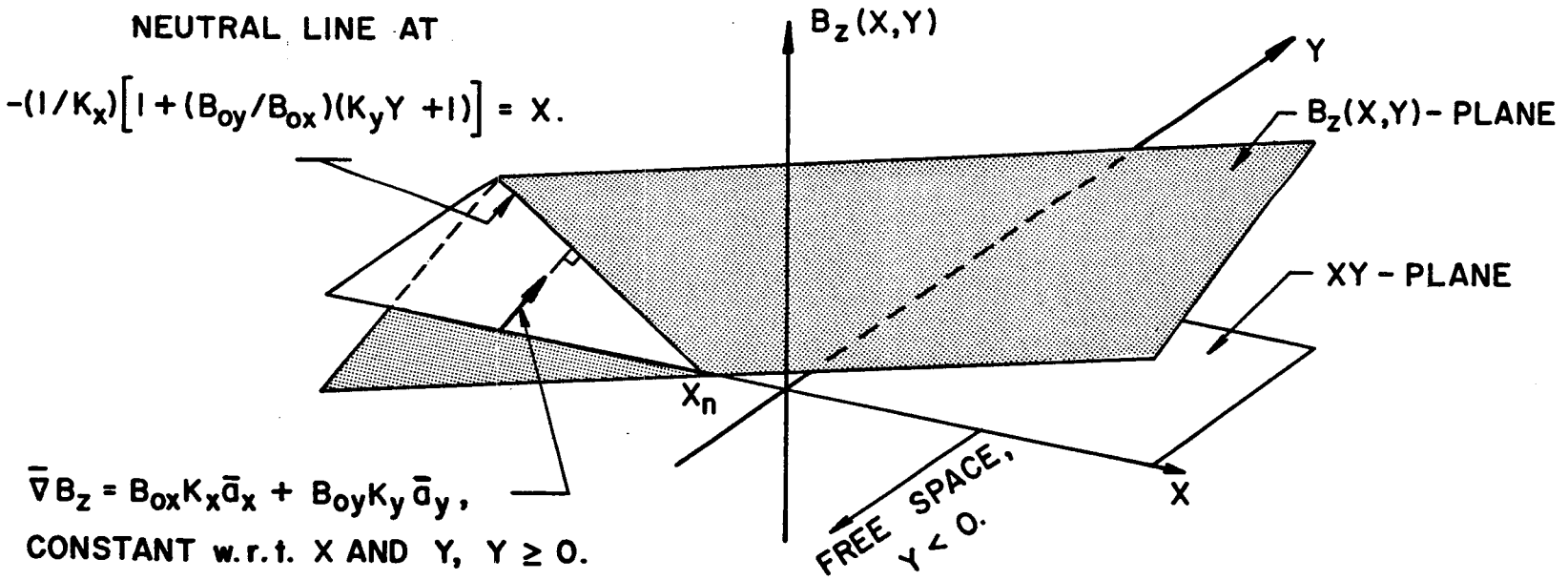

Figure 12. Terminated Magnetic Field With a Non-normal Gradient.

$$\bar{B}_z (X, Y) = \left\{ B_{cx} (K_x X + 1) + B_{oy} (K_y Y + 1) \right\} \bar{a}_z, \quad Y \geq 0,$$

$$= 0, \quad Y < 0, \tag{4.1}$$

where B_{ox}, B_{oy}, K_x and K_y are all positive constants.

This particular field configuration is not meant to be a close model of the actual field near the magnetospheric boundary. Indeed, not much is known about the nature of the magnetic field in the vicinity of the magnetopause. Rather, it is hoped that by investigating particle motion in the terminated field shown in Figure 12, some credulity may be lent to the possibility that charged particles may enter the magnetosphere by drifting perpendicular to a field gradient that is not normal to the magnetospheric boundary. Therefore, since the credibility of this penetration mechanism is the object of this investigation, a detailed quantitative analysis has no significance and will not be carried out.

4.2 Analog Simulation of the Equations of Motion

By using Equations (3.5) and (3.6), which were derived from the Lorentz force equation and Newton's second law, together with the following two relationships,

$$V_x = dX/dt, \tag{4.2}$$

$$V_y = dY/dt, \tag{4.3}$$

one finds that

$$-(q/m)\,(dX/dt)\,B_z = d^2Y/dt^2, \tag{4.4}$$

$$(q/m)\,(dY/dt)\,B_z = d^2X/dt^2. \tag{4.5}$$

Therefore, substituting B_z from (4.1) into (4.4) and (4.5) gives

$$-(q/m)\left[(dX/dt)\left\{B_{ox}\,(K_x X + 1) + B_{oy}\,(K_y Y + 1)\right\}\right] = d^2Y/dt^2, \tag{4.6}$$

$$(q/m)\left[(dY/dt)\left\{B_{ox}\,(K_x X + 1) + B_{oy}\,(K_y Y + 1)\right\}\right] = d^2X/dt^2, \tag{4.7}$$

where $Y \geq 0$, and

$$0 = d^2Y/dt^2, \tag{4.8}$$

$$0 = d^2X/dt^2, \tag{4.9}$$

where $Y < 0$. The required boundary conditions are

$$dX(0^+)/dt = V_{ox}, \tag{4.10}$$

$$dY(0^+)/dt = V_{oy},\ V_{oy} > 0, \tag{4.11}$$

$$X(0^+) = X_o, \tag{4.12}$$

$$Y(0^+) = Y_o,\ Y_o < 0, \tag{4.13}$$

where V_{ox}, V_{oy}, X_o, and Y_o are constants.

The equations of motion (4.6) through (4.9) were simulated on an analog computer (EAI Model TR-48), according to well-known techniques, at the Pennsylvania State University.

Figures 13 through 19 show the simulated trajectories of a 40 kev proton for various angles of incidence and magnetic field gradients. In Figures 13 and 14, $B_{ox} = 4 \times 10^{-8}$ weber/m^2, $K_x = 1.38 \times 10^{-6}\ m^{-1} = (|\ e/m\ |\ B_{ox})/|\ \overline{V}\ |$, and $B_{oy} = 0$. In Figures 15, 16, and 17, $B_{ox} = B_{oy} = 4 \times 10^{-8}$ weber/m^2, and $K_x = K_y = 1.38 \times 10^{-6}\ m^{-1}$. And in Figure 18, $B_{ox} = 0$, $B_{oy} = 4 \times 10^{-8}$ weber/m^2, and $K_y = 1.38 \times 10^{-6}\ m^{-1}$. Figure 19 simply shows the trajectory of a 40 kev proton in a terminated constant magnetic field where $|\ \overline{B}\ | = 4 \times 10^{-8}$ weber/m^2 for $Y \geq 0$, and $|\ \overline{B}\ | = 0$ for $Y < 0$.

As illustrated by these figures, the proton motion can be classified according to four types of behavior: (1) the proton impinges at the boundary where the flux density is high, causing it to be reflected back into free space after penetrating about a Larmor radius; (2) the proton strikes the boundary where the flux density is not quite so high, causing it to penetrate indefinitely into the field region by drifting perpendicular to the field gradient; (3) it moves unimpeded into the field region by moving along the neutral line (see Figure 12) of the field; (4) the proton is incident near the neutral point, X_n, with an angle of incidence which is oblique to the field gradient,

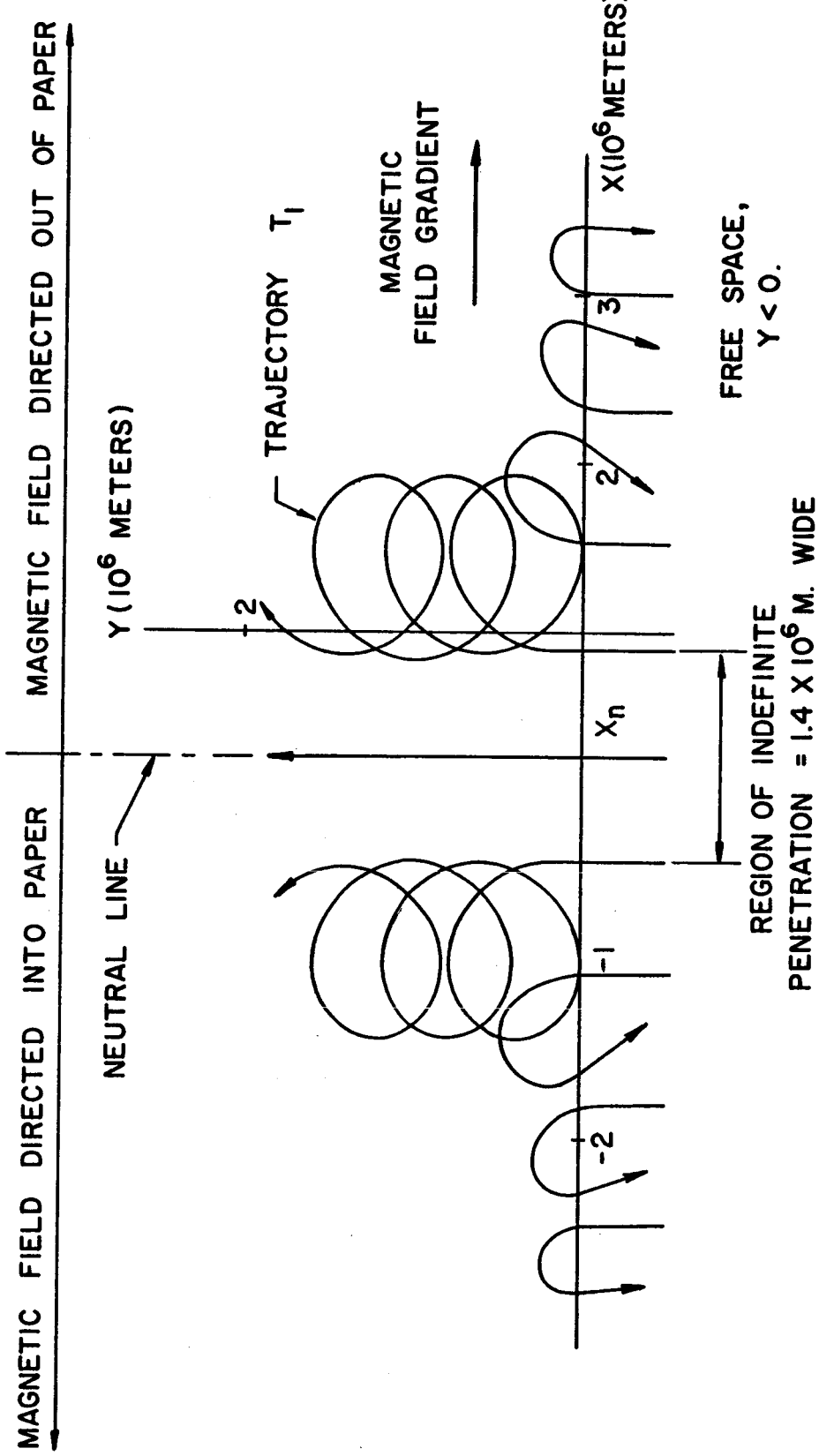

Figure 13. Parallel Gradient and Normal Incidence.

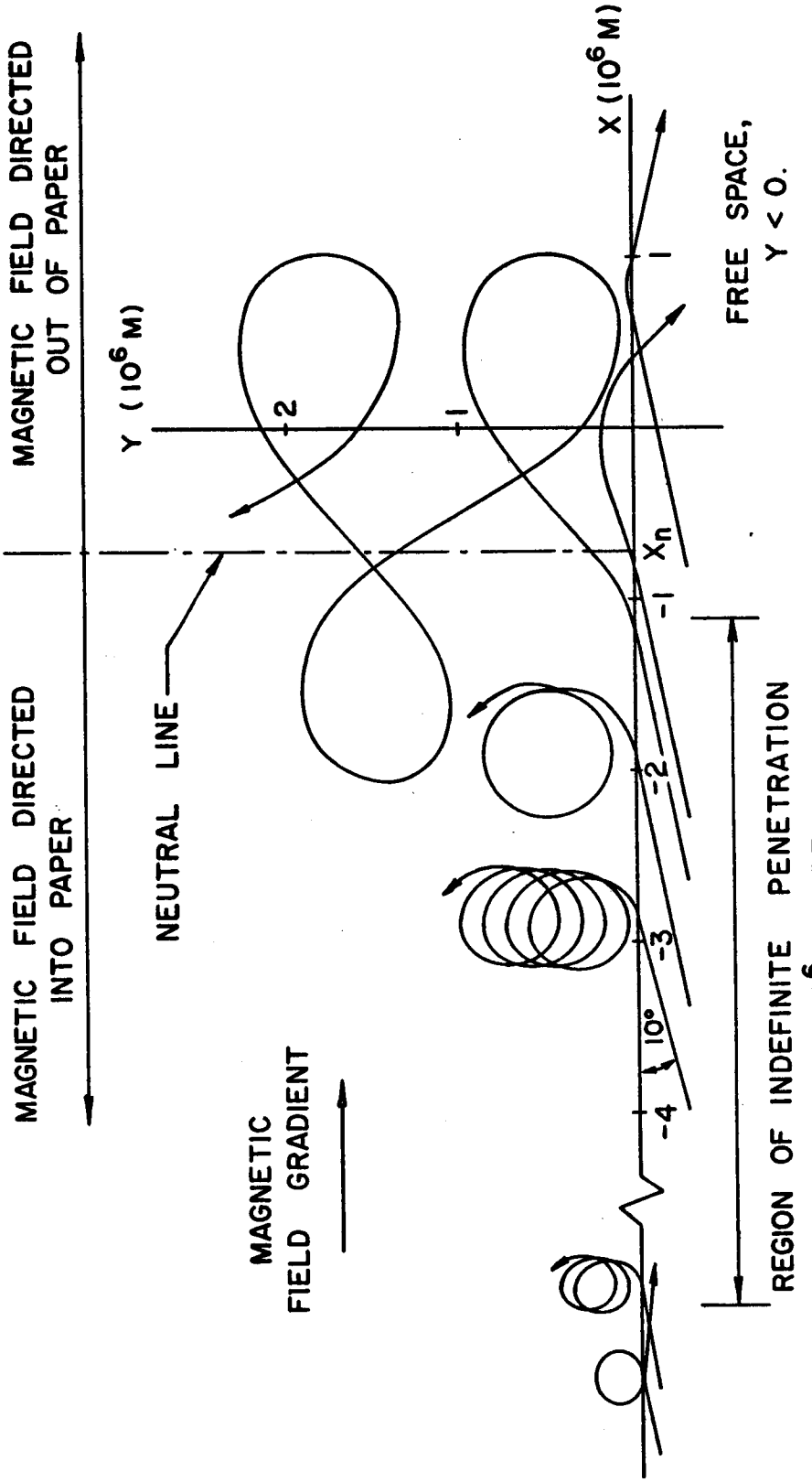

Figure 14. Parallel Gradient and Oblique Incidence.

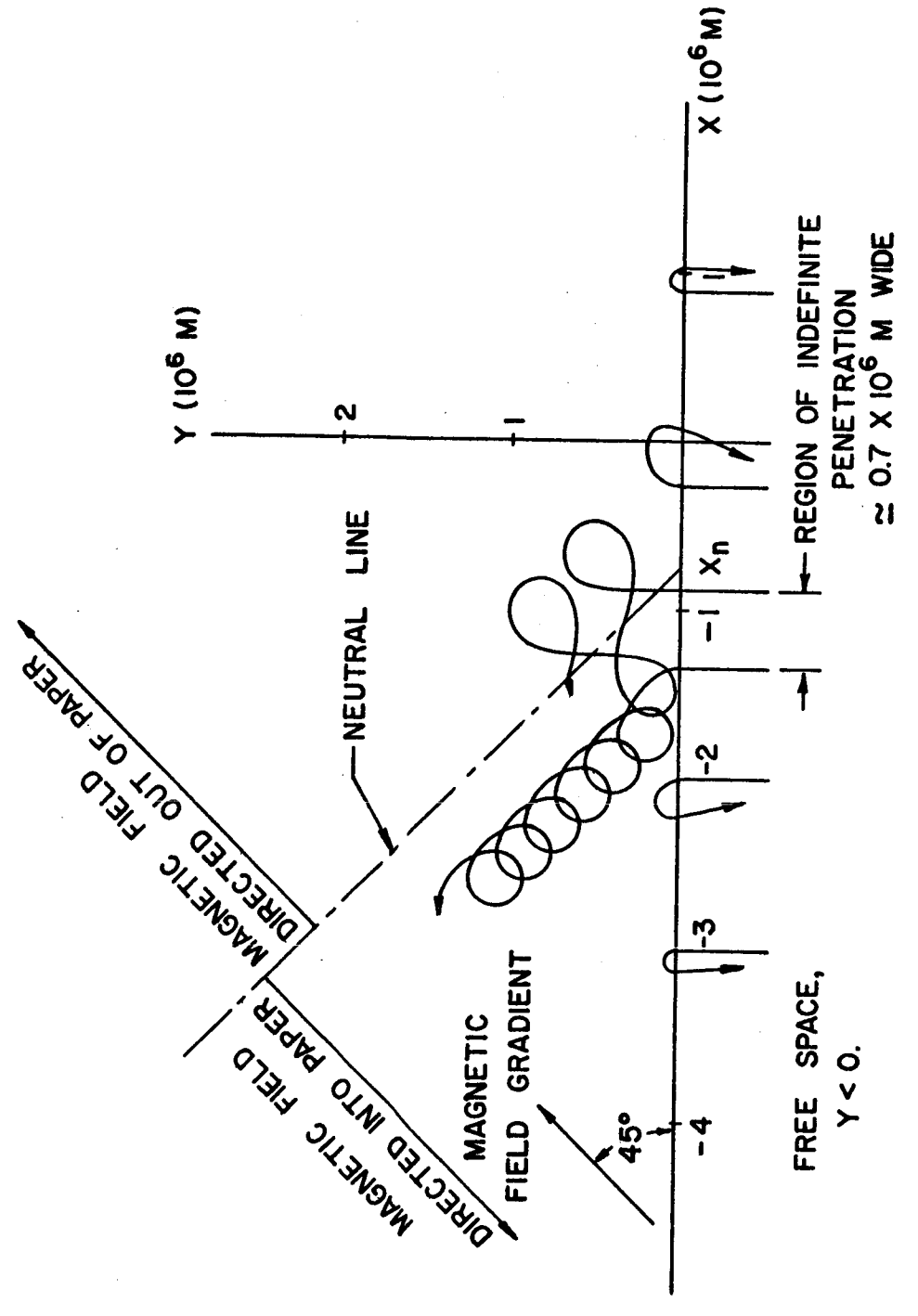

Figure 15. Oblique Gradient and Normal Incidence.

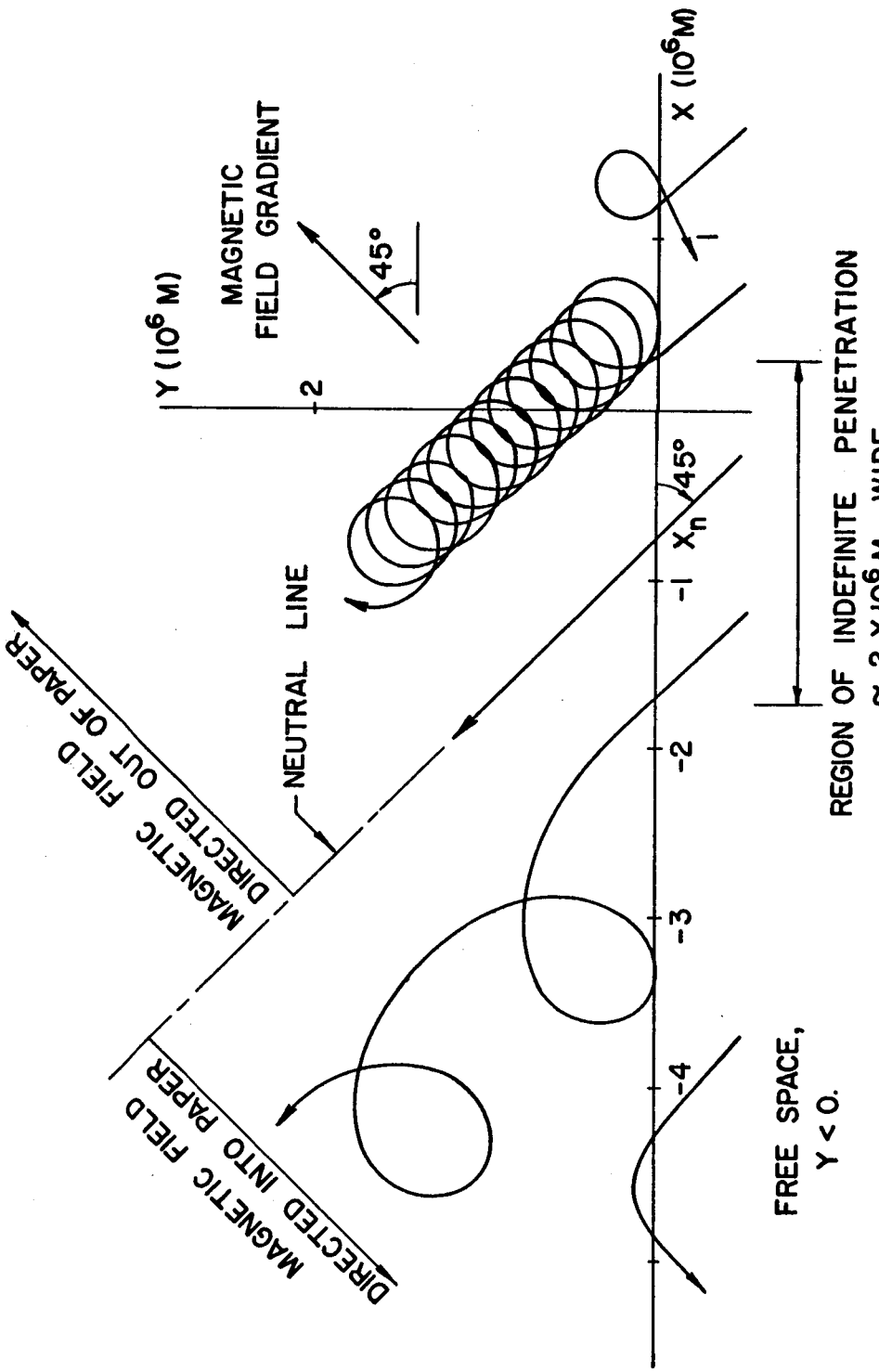

Figure 16. Normal Incidence to an Oblique Gradient

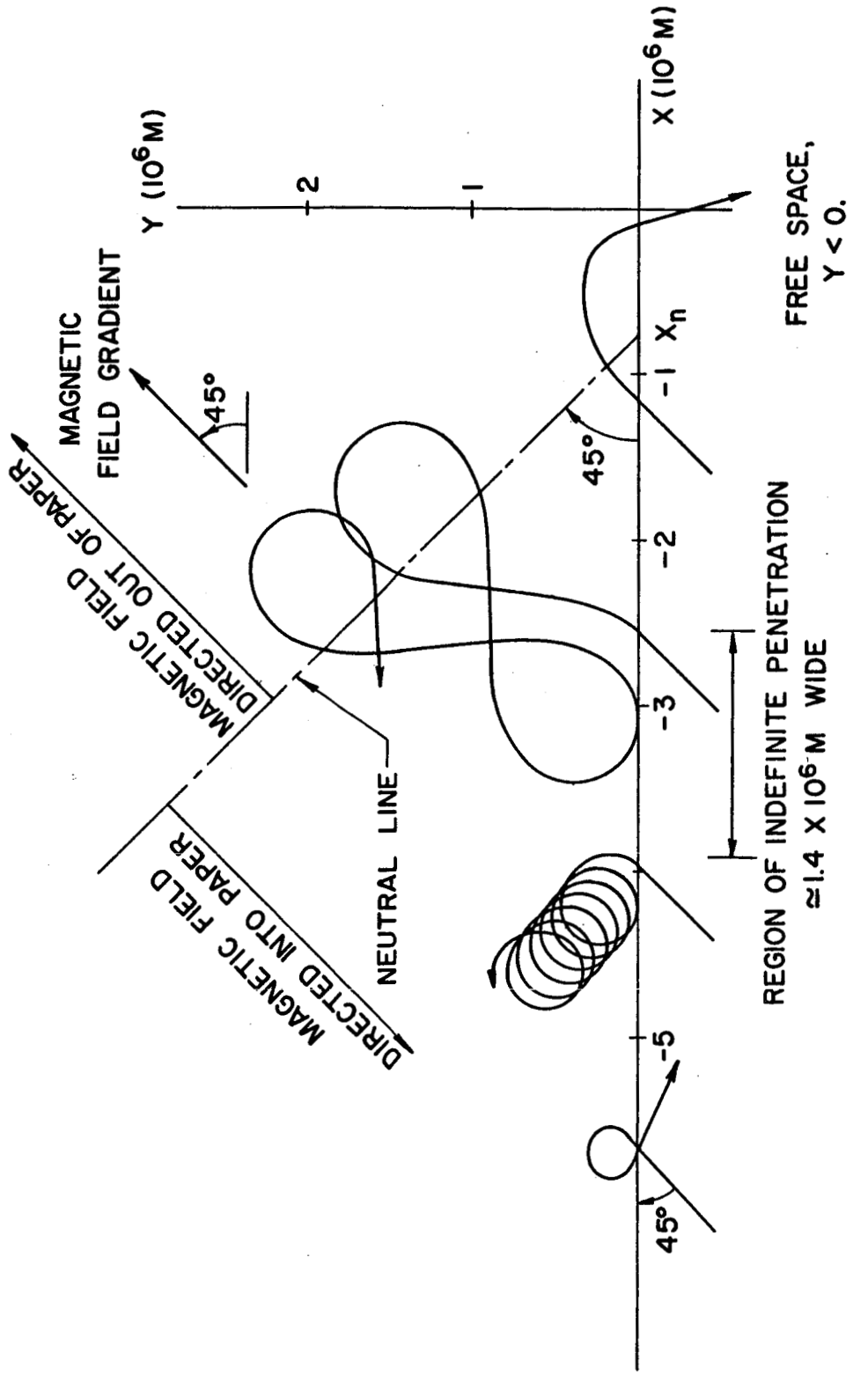

Figure 17. Parallel Incidence to an Oblique Gradient.

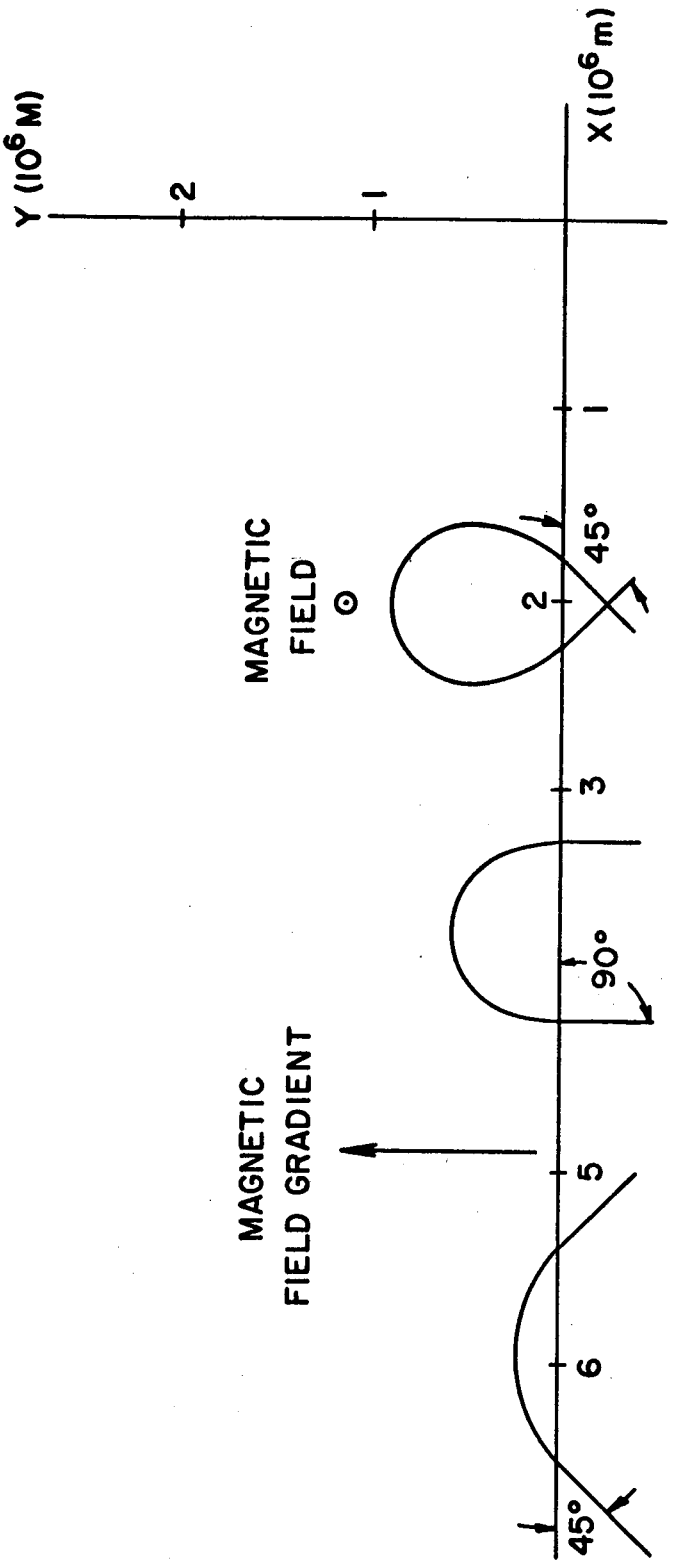

Figure 18. Gradient Normal to Boundary.

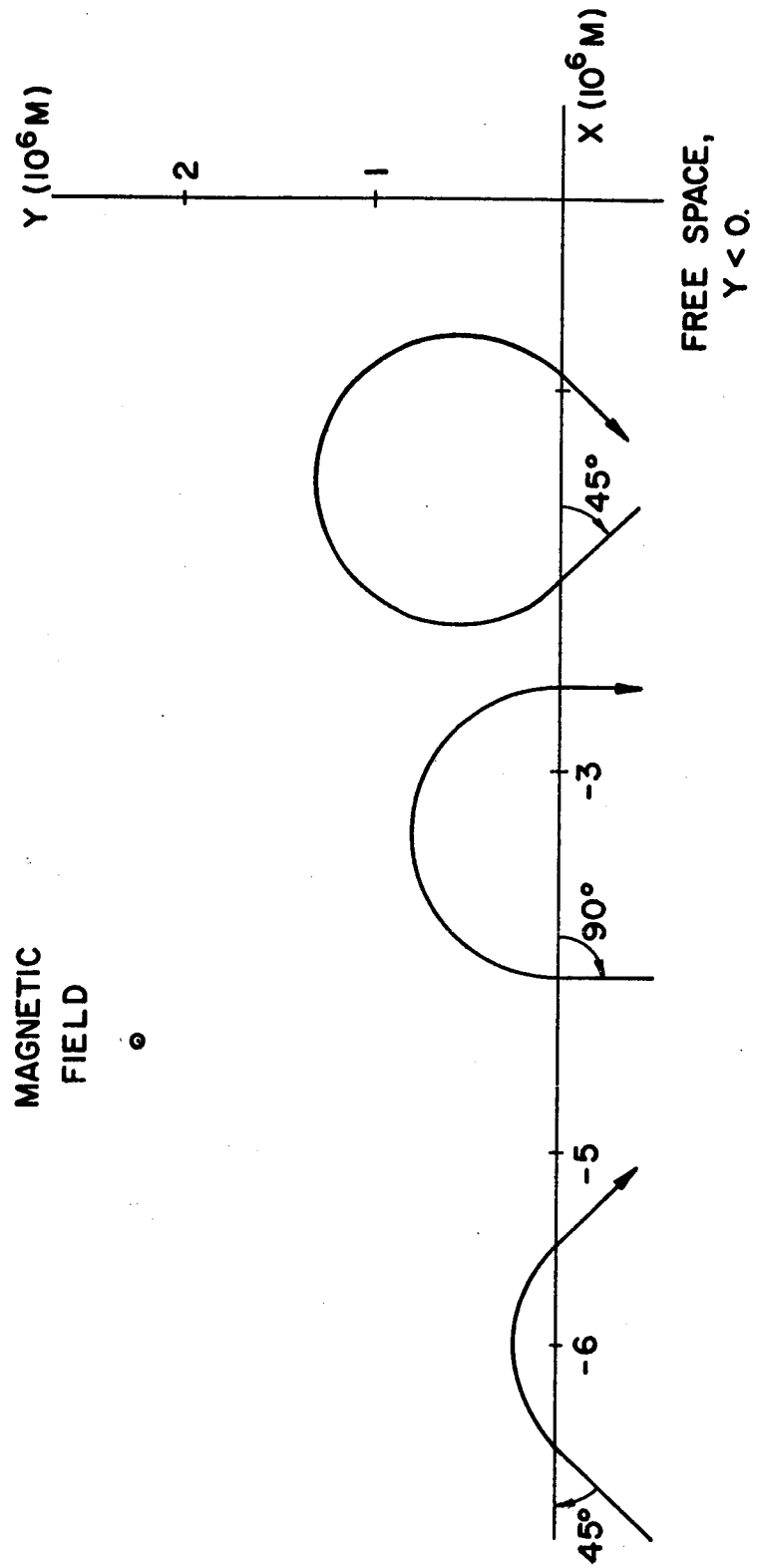

Figure 19. Constant Magnetic Field.

causing the proton to "bounce" back and forth across the neutral line, with an average velocity parallel to the neutral line.

From the analog simulations, it was found that an incident proton may penetrate indefinitely into the magnetic field if it is incident anywhere within a certain vicinity of the neutral point, X_n. Outside this vicinity, however, reflection always occurs because the flux density is so high. Let this vicinity be defined as the region of indefinite penetration. This region is indicated in Figures 13 through 17.

Since the width of the region of indefinite penetration is a measure of the number of protons in an incident proton stream which would enter and stay within the field, it is of interest to investigate how the width varies with angle of incidence, particle energy, particle mass, field gradient, and the scale of the field. Figure 20 shows how the width of the region of indefinite penetration was found to vary with proton energy for the case of normal incidence, where the magnetic field gradient is parallel to the boundary (see Figure 13), and all other parameters are held constant. Figure 21 shows the corresponding variation as a function of the field gradient, $B_{ox} K_x$, for various proton energies, all other parameters being held constant. Due to machine and instrumentation errors, the accuracy of the indicated width of indefinite penetration is about $\pm 0.1 \times 10^6$ meters in these plots. Rather than trying to fit curves to Figures 20 and 21 in order to deduce functional relationships to proton energy and field gra-

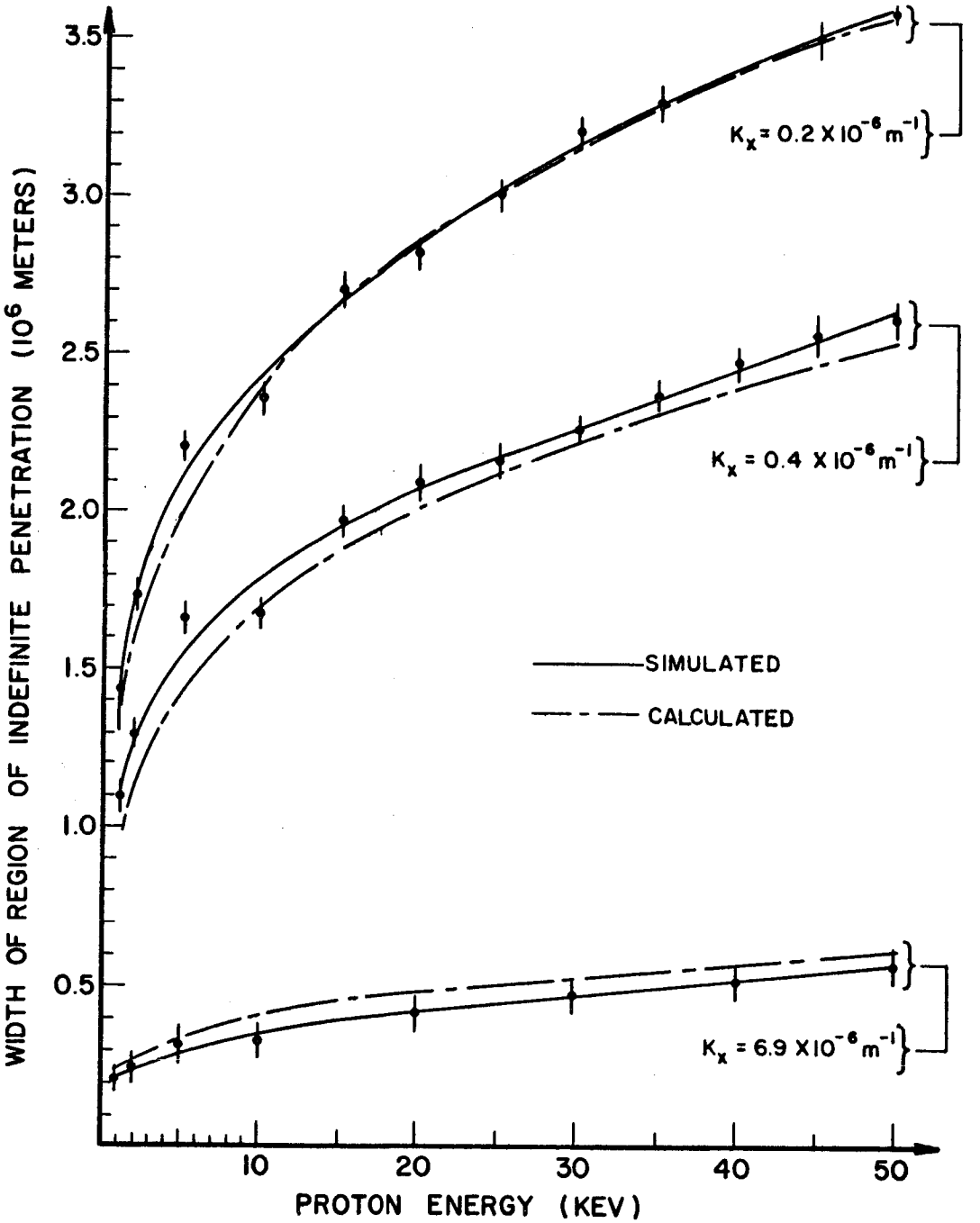

Figure 20. Width of the Region of Indefinite Penetration Versus Proton Energy, for the Case of Normal Incidence and Parallel Gradient.

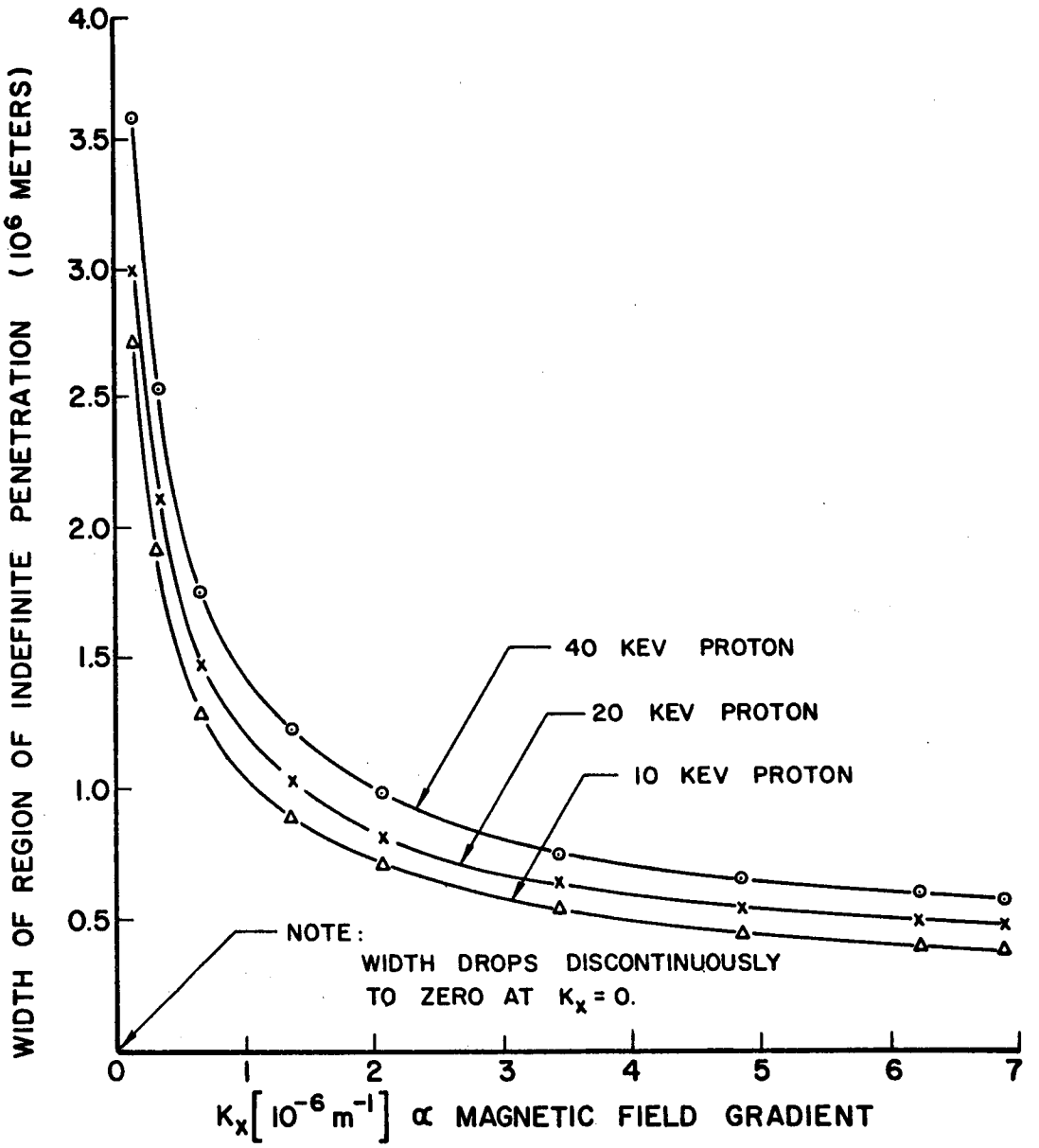

Figure 21. Width of the Region of Indefinite Penetration Versus K_x, for the Case of a Normally Incident Proton and a Parallel Gradient.

dient, adiabatic theory will be employed in the next section to arrive at these dependencies.

From Figures 13 through 21, the following observations may be made.

1.) By Figure 20, when the magnetic field gradient is parallel to the boundary, and the proton is normally incident to the boundary, indefinite penetration may be enhanced by increasing the proton energy, all other parameters being held constant.

2.) By Figure 21, when the magnetic field gradient is parallel to the boundary, and the proton is normally incident to the boundary, indefinite penetration may be enhanced by decreasing K_x, a measure of the magnitude of the field gradient, $B_{ox} K_x$. However, according to Figure 19, when $K_x = 0$, reflection occurs all along the boundary, as expected.

3.) In the case where the magnetic field gradient is parallel to the boundary, comparison of Figures 13 and 14 indicates that indefinite penetration may be enhanced by oblique incidence of the proton, all other parameters being held constant.

4.) For the case of normal incidence, comparison of Figures 13 and 15 indicates that indefinite penetration may be enhanced by decreasing the angle between the magnetic field gradient and the boundary.

5.) For the case where the gradient is oblique to the boundary, comparison of Figures 15, 16, and 17 indicates that indefinite penetration may be enhanced by oblique incidence of the proton.

6.) In agreement with the discussion of Chapter 3, it was found that indefinite penetration could not occur when the magnetic field gradient was normal to the boundary. Figure 19 is an example.

It was also found that by increasing the scale of the field (that is, by increasing B_{ox} or B_{oy}, or both), the width of the region of indefinite penetration could be decreased.

In order to gain some physical insight into what is required for indefinite penetration, the width of the region of indefinite penetration will now be computed by using "first order" theory for the case of normal incidence, where the magnetic field gradient is parallel to the boundary.

4.3 Approximation of the Width of the Region of Indefinite Penetration by First Order Theory

It is well known that the Larmor radius, ρ, of a particle of mass m and charge q in a constant magnetic field of magnitude $|B|$ is given by

$$\rho = \frac{V_{\perp}}{|q/m|\,|B|} \quad , \tag{4.14}$$

where $V_\perp$ is the magnitude of the component of particle velocity which is perpendicular to $\overline{B}$. If a particle moves within a magnetic field which is parallel to the z-axis, but whose strength changes along the x-axis, then as the particle gyrates in the xy plane, its Larmor radius will, according to (4.14), change over the orbit. Such is the case of trajectory T_1 in Figure 13.

According to the "first order" theory developed by Alfvén (1950), if the charged particle experiences small spatial inhomogenieties in $\overline{B}$, the motion of the particle may be described approximately as gyrating around a point which is moving; this instantaneous center of gyration is called the "guiding center" of the particle. And the motion of the guiding center, perpendicular to $\overline{B}$, is termed the "drift" of the particle.

More explicitly, according to Alfvén , if

$$\frac{\nabla_\perp B}{B} \rho \ll 1, \tag{4.15}$$

where $\nabla_\perp B$ is the gradient of the scalar, B, in the plane perpendicular to $\overline{B}$, and ρ is the Larmor radius, then the drift velocity of the guiding center is given approximately by

$$V_D = V_\perp \frac{\rho \nabla_\perp B}{2 B}. \tag{4.16}$$

Figure 22 illustrates indefinite penetration of a proton into the field of Figure 12, for the case of normal incidence, where the magnetic field gradient is parallel to the boundary. Here the magnetic field (scalar) is given by

$$B = B_{ox} (K_x X + 1). \tag{4.17}$$

The motion of an incident proton is obviously symmetric about the neutral line in Figure 22. Therefore, in Figure 22,

$$\begin{aligned} \rho_1 &= \frac{V_\perp}{(q/m)\, B\,(X_1)} \\ &= \frac{V_\perp}{(q/m)\, |\, B\,(X_1')\,|}\,. \end{aligned} \tag{4.18}$$

It will be assumed that (4.15) holds at the end points of the region of indefinite penetration, i.e. at X_1 and X_1'; later on, after X_1 and X_1' have been formally determined by using first order theory, it will be shown that (4.15) does indeed hold.

Inspection of Figure 22 shows that the condition for indefinite penetration at the end point of the region of indefinite penetration, X_1, is given approximately by

$$\rho_1 = V_D\,(3/4)\,\tau, \tag{4.19}$$

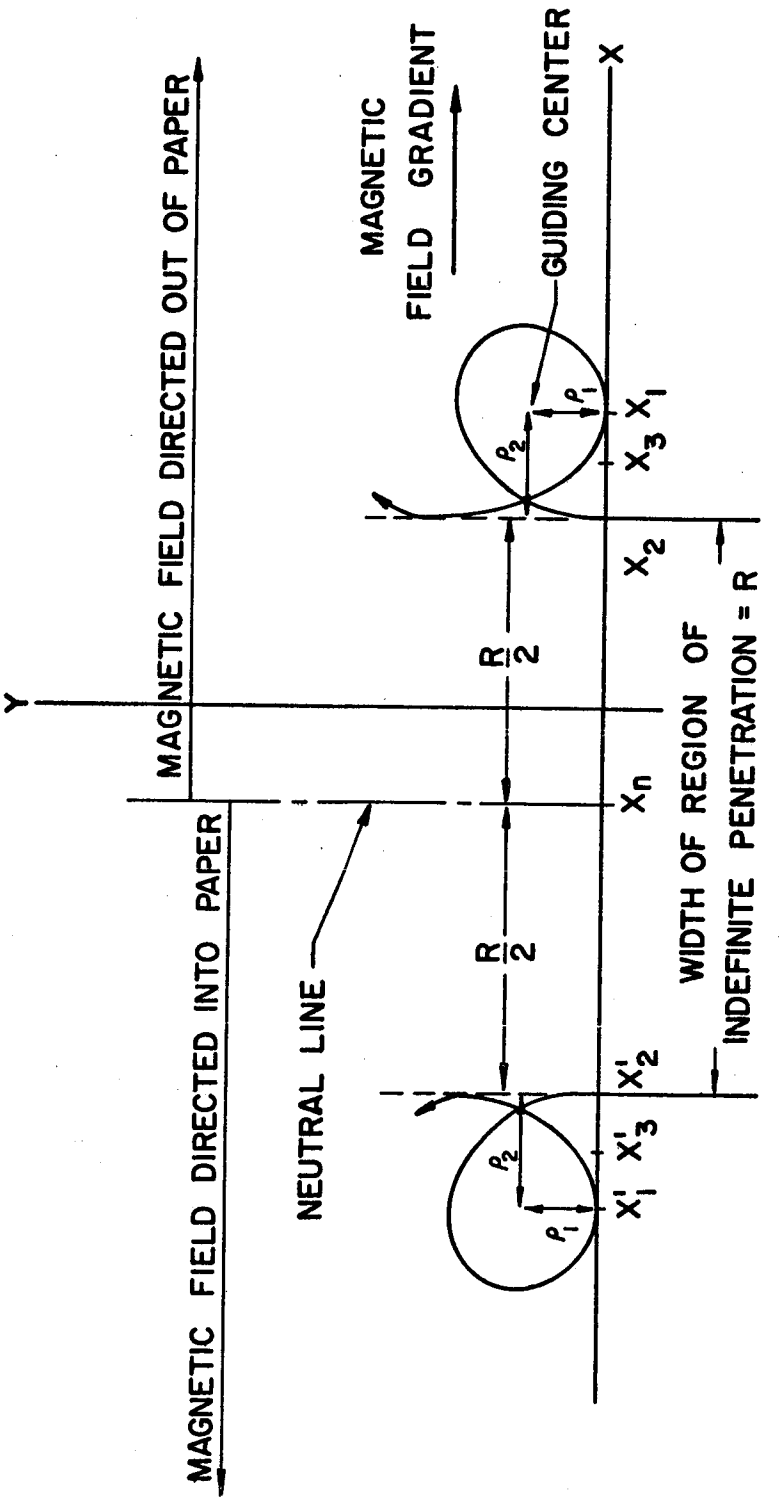

Figure 22. Drift Motion of a Proton at the End Points of the Region of Indefinite Penetration.

where

$$\tau = \frac{2\pi}{(q/m)\, B(X_1)}, \tag{4.20}$$

and V_D is the drift velocity of the guiding center of the proton.

By Equations (4.16), (4.17) and (4.20), the condition for indefinite penetration at X_1, given by (4.19), then becomes

$$X_1 = (1/2)\sqrt{\frac{3\pi V_\perp}{B_{ox}K_x(q/m)}} - \frac{1}{K_x}. \tag{4.21}$$

In a similar fashion, it is found that the condition for indefinite penetration at the other end of the region of indefinite penetration, X_1' is given by

$$X_1' = -(1/2)\sqrt{\frac{3\pi V_\perp}{B_{ox}K_x(q/m)}} - \frac{1}{K_x}. \tag{4.22}$$

The end point, X_1, was found by using first order theory. Now it must be determined whether or not first order theory does apply; that is, it must be determined whether or not (4.15) is met. In (4.15), ρ will be evaluated at X_1; that is,

$$\rho = \frac{V_\perp}{(q/m)\, B\,(X_1)}. \tag{4.23}$$

Therefore, by using (4.17), (4.21) and (4.23), one finds that

$$\frac{\nabla_{\perp} B\,(X_1)}{B\,(X_1)}\ \rho\,(X_1) \;=\; \frac{4}{3\,\pi} \;<\; 0.43, \tag{4.24}$$

for all $K_x > 0$. Consequently, (4.15) is met to some degree; therefore, first order theory should give a solution which is at least somewhat close to being correct.

The width of the region of indefinite penetration, R, shall be defined by

$$R \;\equiv\; X_2 - X_2{}'. \tag{4.25}$$

But, by inspection of Figure 22, one finds that

$$X_2 = X_1 - \rho_2, \tag{4.26}$$

and

$$X_2{}' = X_1{}' + \rho_2. \tag{4.27}$$

Therefore, by using (4.21), (4.22), (4.25), (4.26) and (4.27), one finds that

$$R \;=\; \sqrt{\frac{3\,\pi\,V_{\perp}}{B_{ox} K_x (q/m)}} \;-\; 2\,\rho_2. \tag{4.28}$$

Here ρ_2 may be approximated by (see Figure 22)

$$\rho_2 \;=\; \frac{V_{\perp}}{(q/m)\,B\,(X_3)}, \tag{4.29}$$

where $X_3 = X_1 - \rho_2/\alpha$, α a positive constant. (4.30)

By using (4.17), (4.29), and (4.30), one arrives at the following expression:

$$\rho_2 = \frac{(X_1 + 1/K_x) \pm \sqrt{(X_1 + 1/K_x)^2 - 4\, V_\perp / \left\{ \alpha\, B_{ox} K_x (q/m) \right\}}}{(2/\alpha)}. \tag{4.31}$$

Consequently, by combining (4.21) and (4.31), one finds that

$$\rho_2 = (1/4) \sqrt{V_\perp / \left\{ B_{ox} K_x (q/m) \right\}} \left[\sqrt{3\,\pi\,\alpha^2} \pm \sqrt{3\,\pi\,\alpha^2 - 16\,\alpha} \right]. \tag{4.32}$$

Therefore, by using Equations (4.28) and (4.32), one finds that

$$R = \sqrt{\frac{V_\perp}{B_{ox} K_x (q/m)}} \left\{ (1 - \alpha/2)\sqrt{3\,\pi} \pm (1/2)\sqrt{3\,\pi\,\alpha^2 - 16\,\alpha} \right\}. \tag{4.33}$$

Since $\alpha > 0$, and since ρ_2 (as well as R) must be real, then, by (4.32), it is required that

$$\alpha \geq 16/(3\,\pi). \tag{4.34}$$

In addition, it also turns out that for $16/(3\,\pi) \leq \alpha \leq 3\,\pi/(3\,\pi - 4)$,

$$(1 - \alpha/2)\sqrt{3\,\pi} > (1/2) \sqrt{3\,\pi\,\alpha^2 - 16\,\alpha}\ , \tag{4.35}$$

and for $\alpha > 3\pi/(3\pi - 4)$, the inequality in (4.35) is reversed. Therefore, since R is required to be positive, the plus (+) sign in (4.33) must be used when $\alpha > 3\pi/(3\pi - 4)$; and for $16/(3\pi) \leq \alpha \leq 3\pi/(3\pi - 4)$, either sign may be used in (4.33) in order to make R positive.

There are no constraints on α other than (4.34); therefore, α cannot be determined without resorting to either Figure 20 or 21. Comparing the behavior of R predicted by (4.33) with the computer results shown in Figure 20, it turns out that in order for (4.33) to agree with Figure 20 for at least the single case where $K_x = 0.2 \times 10^{-6}$ m^{-1} and the energy of the proton is 25 kev, it is required that

$$(1 - \alpha/2)\sqrt{3\pi} \pm (1/2)\sqrt{3\pi\alpha^2 - 16\alpha} = 1.8;$$

that is,

$$(3\pi\alpha^2 - 16\alpha)/4 = (1.8 - (1 - \alpha/2)\sqrt{3\pi})^2 . \qquad (4.36)$$

Solving (4.36) for α gives $\alpha = 2.75$, which is an allowable value since it is in accordance with (4.34). Consequently, it appears that the width of the region of indefinite penetration in Figure 22, is given approximately by

$$R = 1.8\sqrt{\frac{V_\perp}{B_{ox}K_x(q/m)}} . \qquad (4.37)$$

Plots of (4.37) corresponding to the cases investigated by the computer are shown in Figure 20. The close agreement between the simulated and calculated curves of Figure 20 at least lends support to the behavior of R as predicted by (4.37). According to Equation (4.17), the width of the region of indefinite penetration for the case of a normally incident proton, when the field gradient is parallel to the boundary, is (1) proportional to the fourth root of energy, (2) inversely proportional to the field gradient ($B_{ox} K_x$), and (3) inversely proportional to the scale of the field (B_{ox}). (It is interesting to note that, unlike the general case where the field gradient was normal to the boundary, which was considered in Chapter 3, indefinite penetration is enhanced by small spatial variations of the field.)

By inspection of Figures 14 through 19, cases involving oblique incidence or gradients which are not parallel to the boundary (or both) cannot always be solved by first order theory. Nor is it believed by the author that an analytic solution for the widths of the regions of indefinite penetration for these cases would be of much value. As was mentioned previously, the magnetic field configuration of Figure 12 was not meant to represent the magnetic field near the magnetospheric boundary. Rather, it is the author's hope that by investigating some trajectories of a proton into the field of Figure 12, some credibility could be lent to the possibility that charged par-

ticles may enter the magnetosphere by drifting perpendicular to a field gradient that is not normal to the magnetospheric boundary.

The possibility of energy differentiation by a magnetic field was demonstrated by Figure 20 and Equation (4.37). In addition, since the direction of the cyclotron motion of a charged particle depends upon the sign of its charge, it is apparent that there may also be a differentiation with respect to the sign of the charges of incident particles. Consequently, in the case of the magnetosphere, the field near the boundary could act like a filter--that is, it may allow some charged particles to penetrate deep within it, while rejecting others, simply on the basis of drift motion of the particles. At the present, however, the lack of knowledge of the magnetospheric field on a sufficiently small spatial scale makes it impossible to conclude any such drift motion actually does occur.

CHAPTER 5

SUMMARY AND CONCLUSIONS

This work is a theoretical investigation of the trajectory of a solitary charged particle which emanates from free space and is incident at the boundary of an idealized magnetic field. The object is to arrive at some understanding of what is required of the magnetospheric field if charged particles, incident at the magnetospheric boundary, are to be prevented from being reflected back out of the magnetospheric boundary.

In Chapter 2, the Lorentz force equation and Newton's second law are used to arrive at the equations of motion of a solitary charged particle which is incident along the equatorial plane of a terminated dipole magnetic field. The equations of motion are solved analytically, and it is shown that the incident particle is always reflected back into free space.

Consequently, in Chapter 3, an attempt is made to deduce some static and time-varying, non-dipolar magnetic field variations required for deep penetration and trapping; emphasis is put on the case where the field gradient is normal to the boundary of the terminated field. For the case of the static field, when the field gradient is normal to the boundary, it is shown that the incident charged particle will always be reflected back into free space if the field is monotonically increasing or decreasing; but the particle may penetrate deep within the field

if large non-montonic variations in flux density occur over a Larmor radius--localized field reversals being an obvious example.

Also, for the case when the field gradient is normal to the boundary, an example of particle trapping due to time variations of the flux density is given in Section 3.2. As pointed out in this example, however, the time scale involved is of the order of a Larmor period (e.g., about 2 seconds for a proton in a field of 3×10^{-8} weber/m^2) -- a period much smaller than the presently known temporal variations of the magnetospheric field (see Cahill and Amazeen, 1963).

Then, in Chapter 4, analog simulation is employed to show that a charged particle may penetrate indefinitely into a terminated field by drifting perpendicular to a magnetic field gradient, provided the gradient is not perpendicular to the boundary of the field. In particular, using the terminated field of Figure 12 (together with reasonable parameters), it is shown that the transmissibility of the particle at the boundary is determined by (1) the energy of the particle, (2) the angle of incidence of the particle, (3) the scale of the field, and (4) by the angle between the field gradient and the boundary (see Figures 13 through 21). In addition, first order theory is used to arrive at an analytic expression for the width of the region of indefinite penetration (defined on pp. 66), for the case where the field gradient is parallel to the boundary and the particle is

a normally incident proton; this expression, Equation (4.37), is found to be in good agreement with the results of the analog simulations (see Figure 20).

This investigation of the trajectories of a proton into the terminated field of Figure 12 is intended to lend some credibility to the possibility that charged particles may enter the magnetosphere by drifting perpendicular to a magnetic field gradient which is not normal to the magnetospheric boundary. In the case of the magnetosphere, this probably could be a local type of phenomenon, at best, in the low latitude regions of the sunside of the magnetosphere, since the macroscopic behavior of the magnetospheric field is known to have a strong radial dependence in this region (see Cahill and Amazeen, 1963).

Matuura and Nagata (1960) also considered a terminated magnetic field, making mention of the importance of the direction of the magnetic field gradient in affecting the transmissibility of the particle at the boundary. In addition, they argued that once passed the boundary, charged particles may possibly take a "randon walk" into the magnetosphere due to irregularities in the magnetic field (the mean life of an individual irregular structure being assumed to be of the order of 10 seconds--a period considerably longer than the Larmor period of the particles considered).

At the present, however, the lack of knowledge of the

magnetospheric field on a sufficiently small spatial and time scale (see Fairfield and Ness, 1966), makes it impossible to conclude that localized behavior of the magnetic field along the magnetospheric boundary may actually be a key factor in contributing to deep particle penetration of the magnetosphere.

In the event that more is learned about the field near the magnetospheric boundary, a suggestion for further study would be to simulate a more realistic model in an attempt to confirm whether direct penetration of charged particles across the magnetospheric boundary is possible.

APPENDIX A

Given: A single particle of charge q, mass m, and velocity $\overline{V}$, moves within an arbitrary pure magnetic field, $\overline{B}$.

To Prove: i) $|\overline{V}|^2 = K_o$, a constant, and

ii) $dm/dt = 0$.

Proof:

i) By using the Lorentz force equation, $\overline{F} = q(\overline{V} \times \overline{B})$, and Newton's second law, $\overline{F} = d(m\overline{V})/dt$, one finds that

$$q(\overline{V} \times \overline{B}) = \overline{V}\,(dm/dt) + m\,(d\overline{V}/dt). \tag{A.1}$$

But since $\overline{V}$ and $(\overline{V} \times \overline{B})$ are orthogonal,

$$q\,\overline{V} \cdot (\overline{V} \times \overline{B}) = 0. \tag{A.2}$$

Therefore, by (A.1) and (A.2),

$$0 = \overline{V} \cdot \left\{ \overline{V}\,(dm/dt) + m\,(d\overline{V}/dt) \right\}$$

$$= |\overline{V}|^2 (dm/dt) + m\,\overline{V} \cdot (d\overline{V}/dt)$$

$$= |\overline{V}|^2 (dm/dt) + (m/2)\,(d\,|\overline{V}|^2/dt). \tag{A.3}$$

Therefore, by (A.3),

$$2\,(dm/m) = -\,(d\,|\overline{V}|^2/|\overline{V}|^2). \tag{A.4}$$

Integrating (A.4) gives

$$\log_e (m|\overline{V}|^2) = C_o, \text{ a constant.} \qquad (A.5)$$

But the mass, m, is a function of the velocity of the particle, increasing with increasing speed according to the relation

$$m = m_o/\sqrt{1 - (|\overline{V}|^2/c^2)}, \qquad (A.6)$$

where c is the speed of light, and m_o is the "rest mass" of the particle.

Therefore, by using (A.5) and (A.6), one finds that

$$\log_e\left\{ m_o |\overline{V}|^2/\sqrt{1 - (|\overline{V}|^2/c^2)} \right\} = C_o, \qquad (A.7)$$

which implies

$$|\overline{V}|^2 = K_o, \text{ a constant.} \qquad (A.8)$$

Q. E. D.

ii) Since $|\overline{V}|^2$ is a constant,

$$d|\overline{V}|^2 = 0. \qquad (A.9)$$

Therefore, by (A.4) and (A.9),

$$dm = 0, \qquad (A.10)$$

which implies

$$dm/dt = 0. \qquad (A.11)$$

Q. E. D.

BIBLIOGRAPHY

Alfvén, H., and C. Falthammer, Cosmical Electrodynamics, Oxford Press, 1963.

Allen, C. W., Mon. Not. R. Astr. Soc., 106, 137, 1946.

Biermann, L., Z. Astrophys., 29, 274-286, 1951. Cited by W. N. Hess, G. D. Mead, and M. P. Nakada, Rev. Geophys., 3, 521-570, 1965.

Birkeland, K., Arch. Sci. Phys. Nat., 1, 497, 1896. Cited by T. W. Speiser, Scientific Report No. 222, Ionosphere Research Laboratory, The Pennsylvania State University, October 10, 1964.

Blackwell, D. E., Mon. Not. R. Astr. Soc., 116, 56, 1956.

Block, L. P., Report No. 65-10, Royal Institute of Technology, Stockholm, 1965.

Blum, R. Icarus, 1, 459-488, 1963.

Bonetti, A., H. S. Bridge, A. J. Lazarus, B. Rossi, and F. Scherb, J. Geophys. Res., 68, 4017-4063, 1963.

Bridge, H., A. Egirdi, A. Lazarus, E. Lyon, and L. Jacobson, Space Res., 5, 969-978, 1965.

Cahill, L. J., and P. J. Amazeen, J. Geophys. Res., 68, 1835-1843, 1963.

Chamberlain, J. W., Astrophys. J., 131, 47-56, 1960.

Chapman, S., and V. C. A. Ferraro, Terrest. Mag. and Atmos. Elec., 36, 77-97, 171-186, 1931.

Chapman, S., and V. C. A. Ferraro, Terrest. Mag. and Atmos. Elec., 37, 147-156, 421-429, 1932.

Chapman, S., and V. C. A. Ferraro, Terrest. Mag. and Atmos. Elec., 38, 79-96, 1933.

Coleman, P. J., Jr., Leverett Davis, Jr., and C. P. Sonett, Phys. Rev. Letters, 5, 43-46, 1960.

Dungey, J. W., Scientific Report No. 69, Ionosphere Research Laboratory, The Pennsylvania State University, September 15, 1954.

Dungey, J. W., Cosmic Electrodynamics, Cambridge University Press, Cambridge, 1958.

Dungey, J. W.,Phys. Rev. Letters, 6, No. 2, 47, January 15, 1961.

Fairfield, D. H., and N. F. Ness, Report No. X-612-66-530, Goddard Space Flight Center, Greenbelt, Md., November, 1966.

Giovanelli, R. G., Mon. Not. R. Astr. Soc., 107, 338,1947. Cited by T. W. Speiser, Scientific Report No. 222, Ionosphere Research Laboratory, The Pennsylvania State University, October 10, 1964.

Grebowsky, J. M., Scientific Report No. 277, Ionosphere Research Laboratory, The Pennsylvania State University, July 30, 1966.

Gringauz, K. I., V. V. Bezrukikh, V. D. Ozerov, and R. E. Rybchinskii, Dokl. Acad. Nauk. SSSR, 131, 1301, Soviet Phys. Dokl., 5, 361-364, 1960. Cited by W. N. Hess, G. D. Mead, and M. P. Nakada, Rev. Geophys., 3, 521-570, 1965.

Hale, G. E., Astrop. J., 38, 27-98, 99-125, 1913.

Hale, G. E., F. H. Sears, A. Van Maanen, and F. Ellermann, Astrop. J., 47, 206-254, 1918.

Hess, W. N., G. E. Mead, and M. P. Nakada, Rev. Geophys., 3, 521-570, 1965.

Hones, E. W., and J. E. Bergeson, J. Geophys. Res., 70 4951-4958, October, 1965.

Hoyle, F., Some Recent Researches in Solar Physics, Cambridge University Press, Cambridge, 1949.

I. G. Bulletin 84, Trans. Am. Geophys. Union, 45, 501-520, 1964.

Kelvin, Proc. R. Soc., 52, 307-308, 1892. Cited by S. Chapman and V. C. A. Ferraro, Terrest. Mag. and Atmos. Elec., 36, 77, 1931.

Matuura, N., and T. Nagata, Rep. Ionos. Res. Japan, 14, 259-272, September, 1960.

Maxwell, J. C., Electricity and Magnetism, Vol. II, 2nd ed., pp. 263-275, Clarendon Press, Oxford, 1881. Cited by S. Chapman and V. C. A. Ferraro, Terrest. Mag. and Atmos. Elec., 36, 176, 1931.

Ness, N. F., J. Geophys. Res. 70, 2989, 1965.

Parker, E. N., Astrophys. J., 128, 664-676, 1958.

Parker, E. N., Astrophys. J., 132, 821-866, 1960.

Parker, E. N., Interplanetary Dynamical Processes, Interscience Publishers, Inc., 1963.

Speiser, T. W., Scientific Report No. 222, Ionosphere Research Laboratory, The Pennsylvania State University, October 10, 1964.

Spitzer, L., Jr., Physics of Fully Ionized Gases, Interscience Publishers, Inc., New York, 1956.

Störmer, C., The Polar Aurora, Clarendon Press, Oxford, 1955.

Van Allen, J. A., State Univ. Iowa Rept. SUI 60-13, 1960.

White, R. S., Physics Today, 19, 25-38, October, 1966.